UNIVERSITY OF THE WEST of SCOTLAND

UWS

Hochschule für Angewandte Wissenschaften Hamburg

Hamburg University of Applied Sciences

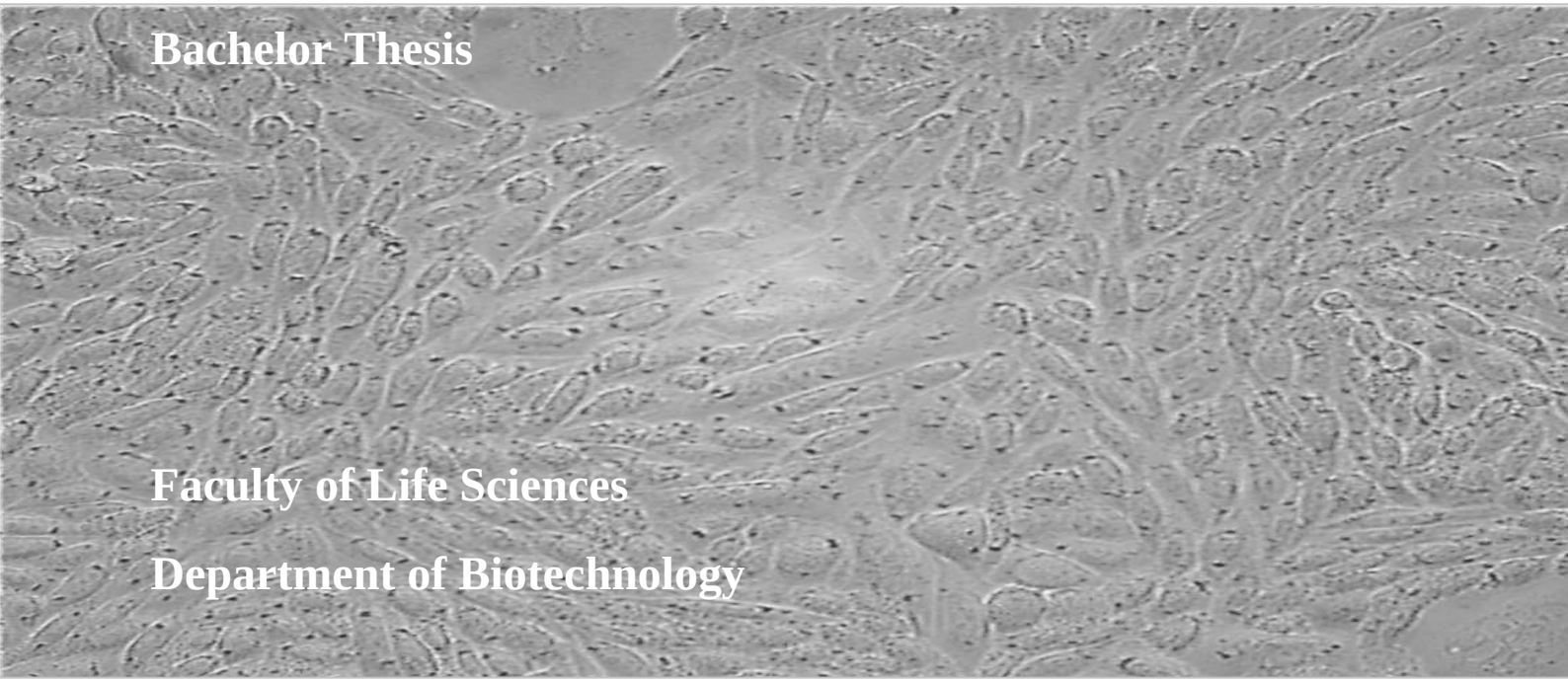

Bachelor Thesis

Faculty of Life Sciences

Department of Biotechnology

Production of Recombinant Receptor Activator of Nuclear Factor κ B Ligand for *in vitro* Osteoclastogenesis

Silke Machauer

February 20th 2013

This work is dedicated to all those wonderful friends

who made studying Biotechnology the best decision of my life.

Statutory Declaration

I hereby assure that this thesis is a result of my personal work and that no other than the indicated aids have been used for its completion. Furthermore I assure that all quotations and statements that have been inferred literally or in a general manner from published or unpublished writings are marked as such. Beyond this I assure that the work has not been used, neither completely nor in parts, to pass any previous examination.

_____

Hamburg, February 20th 2013
Silke Machauer

Abstract

Receptor Activator of Nuclear Factor κ B Ligand (RANKL) is a protein that belongs to the family of tumour necrosis factors (TNF) and is one of the two main inducers of osteoclast differentiation. It is therefore used in research facilities that study the molecular and cellular backgrounds of osteoarthritis (OA), a degenerative bone disease that is thought to be associated with a decline in osteoclast number or function. The aim of this work was to produce RANKL, using classical as well as novel methods and techniques of molecular biology and cell culture, including screening for the gene *RANKL* in leukaemic cell lines, amplification, transformation of *Escherichia coli* (*E. coli*) with a plasmid in which *RANKL* was previously inserted and subsequent analysis of clones, transfection of Chinese Hamster Ovary (CHO) cells with the purified plasmid, and finally qualitative and quantitative analysis of the protein RANKL in the supernatant of a transfected CHO culture.

Contents

Abbreviations

AP-1	Activator Protein 1
BSA	Bovine Serum Albumin
cDNA	Complementary DNA
CFU	Colony Forming Units
CHO	Chinese Hamster Ovary
CMS	Centre for Musculoskeletal Science
C_T	Threshold Cycle
Easy-A	Easy-A Hi-Fi PCR Cloning Enzyme (Agilent Technologies)
E. coli	*Escherichia coli*
FBS	Foetal Bovine Serum
FRT	Flp Recombination Target
GoTaq	GoTaq® DNA Polymerase (Promega)
LB	Luria-Bertani
MCS-F	Macrophage Colony-Stimulating Factor
NFATc1	Nuclear Factor of Activated T-Cells, cytoplasmic 1
NFκB	Nuclear Factor κ B
OA	Osteoarthritis
OPG	Osteoprotegerin
PAR-2	Protease-Activated Receptor 2
PCR	Polymerase Chain Reaction
qRT-PCR	Quantitative Real-Time Polymerase Chain Reaction
RANK	Receptor Activator of Nuclear Factor κ B
RANKL	Receptor Activator of Nuclear Factor κ B Ligand
RT	Reverse Transcription
RQ	Relative Gene Expression compared to a control sample
TE	Transformation Efficiency
TNF	Tumour Necrosis Factor
TNF-α	Tumour Necrosis Factor α
TRAP	Tartrate-Resistant Acid Phosphatase

1. Introduction

Osteoarthritis (OA) is a degenerative joint disease that leads to pathological alterations of cartilage and subchondral bone; for a long time, OA was considered to be a typical 'wear and tear' symptom of old age, as the disease is particularly common in the elderly population. During the past twenty years however, it has become known that OA is more than just that. Environmental factors, lifestyle, genetic predisposition, alterations in gene expression and immunological influences can all contribute to OA (Sharma and Kapoor, 2007; Karsenty and Wagner, 2002).

One characteristic of OA is osteosclerosis, which involves osteoclasts, bone cells resorbing bone tissue, and it is likely that a decrease in number or alteration in function of these particular cells is connected to the disease (Xing et al., 2005). Protease-activated receptor 2 (PAR-2) is a receptor that is present on many different cell types (Smith et al., 2004), but it could also be determined on the surface of osteoclasts and osteoclast progenitor cells (Freeburn, 2012).

The Centre for Musculoskeletal Science (CMS) is a partnership between the School of Science at the University of the West of Scotland and the Institute of Infection, Immunity and Inflammation at the University of Glasgow. One of the main focuses of CMS is to investigate the exact role of PAR-2 on osteoclasts and its contribution to osteoclastogenesis.

Osteoclasts can be grown *in vitro* by separating monocytes from human blood and then cultivating them in the presence of RANKL and further supplements (Khosla, 2001). Recombinant RANKL is openly available, but it represents an enormous cost factor. For this reason, the aim of this work was to find a way to produce it in a more cost effective manner, using the local facilities.

2. Theoretical Background

As this work was conducted in a research group that deals with OA, it was first of all necessary to get familiar with the disease itself and the cellular as well as molecular backgrounds of its development. This chapter is therefore recapitulating the current state of knowledge concerning osteoarthritis and osteoclastogenesis. Additionally, important facts about RANKL and special methods that were used for this work are illustrated.

2.1 Osteoarthritis – The Disease in General

Osteoarthritis, the most common form of arthritis, is a degenerative joint disease that affects mainly the articular cartilage and the subchondral bone. Typically affected are the knees, hips, and fingers, however there is no limitation concerning the diseased joints as OA can occur on every kind of synovial joint. Clinical symptoms are usually swollen and deformed joints, also stiffness and pain when moving or loading the affected limbs (Sharma and Kapoor, 2007).

OA is one of the main reasons for chronic disability in today's society; according to a report from the World Health Organization (WHO), approximately 151.4 million people worldwide were afflicted with OA in 2004. Assuming a total population of 6.5 billion, this is equivalent to 2.3 % of the world's population. Of these patients, 43.4 million, almost one third, were suffering from moderate to severe disability because of their physical condition (WHO, 2008). The high number of OA patients is not only a medical problem, there are also economic consequences as the increasing costs for medical treatment and disability care financially affect society.

Over 50 year olds and especially postmenopausal women are more likely to develop OA, basically the probability increases with age, however, younger people can also develop OA. There is a gender-related dependence of developing OA, for instance, women are more likely

to develop knee OA than men of the same age, whereas there are less differences between men and women concerning hip OA. Another important factor is genetic susceptibility, as especially onset of the disease at lower age seems to be heritable (Sharma and Kapoor, 2007).

In addition to these systemic influences, there are local risk factors that can lead to permanent damage of the joint structures, such as joint injuries, obesity and other forms of excessive joint loading, for instance, jackhammer operators have a relatively high risk for developing hip OA because the hip joints act as shock absorbers in this particular work (Felson, 2003).

In order to understand the pathological changes that go on in a diseased joint, it is important to first understand a healthy one. A joint is formed where two or more bones meet. There are three different types of joints that are found in the mammalian body: Fibrous, cartilaginous and synovial joints, however, only the latter can be affected by OA, the following description therefore refers to this kind of joint.

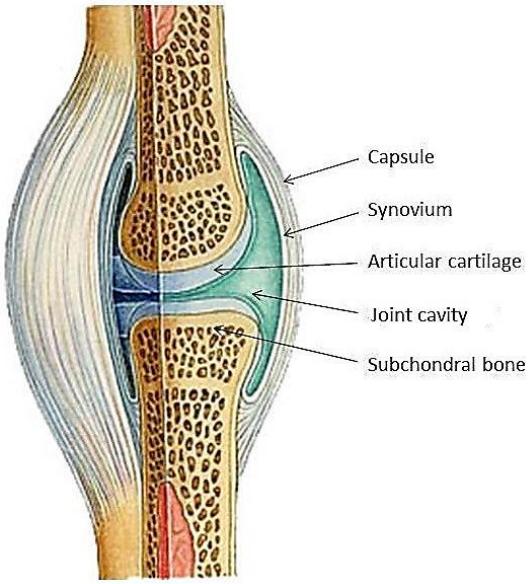

Figure 1 The components of a healthy synovial joint that are affected in osteoarthritis.
adapted from:
Synovial Joint – Free Clip Art – DK Books. URL: http://www.clipart.dk.co.uk/1217/subject/Biology/Synovial_joint [Accessed: 19.09.2012]

Figure 1 shows the joint cavity between two bones which is enclosed by the synovium (synovial membrane) and the fibrous capsule. The synovium secretes the so-called synovial fluid into the joint cavity. This fluid contains nutrients and lubricates the joint. The bone ends are covered by articular cartilage (Kingston, 2000).

The articular cartilage primarily consists of collagen (mainly type II), negatively charged proteoglycan, and a comparably small number of specialized cells, the chondrocytes (Poole et al., 2007). Fibres made of collagen molecules form the characteristic network in the extracellular matrix by arranging themselves in specific patterns depending on their distance to the nearest chondrocytes. In contrast to bone tissues, neither cartilage nor the synovial fluid contains blood vessels; nutrients for the chondrocytes are therefore provided by diffusion (Heinegård et al., 2003). Pathologic alterations due to OA occur to all tissues represented in Figure 1.

The subchondral bone is primarily affected by an increased bone turnover; when the homoeostasis between bone formation and degradation is off balance[1], this can lead to subchondral bone cysts and the formation of osteophytes, which are bone appendages on the edges of the subchondral bone (Poole et al., 2007).

The degradation of cartilage is the most pivotal symptom of OA; it is provoked by increased activity of metalloproteinases and other proteinases that cleave cartilage components such as collagen II and proteoglycans. In addition, the chondrocytes of diseased cartilage show an augmented expression of receptors for interleukin IL-1 and tumour necrosis factor α (TNF-α). Both ligands play an important role in inflammation processes and additionally act as activators of cartilage degradation (Goldring, 2000).

[1] See chapter 2.2 for further information

Furthermore, diseased joints show a thickened capsule and evidence of an inflamed synovium, a symptom called synovitis. However, this pathological condition is more characteristic for rheumatoid arthritis. In fact, OA related synovitis is considered to be associated with crystallisation of calcium salts, whereas rheumatoid arthritis is a systemic inflammatory disorder (Poole et al., 2007).

As cartilage does not absorb X-rays, only pathological alterations concerning the bone can be determined by a radiogram. The narrowing of the joint cavity as a result of cartilage breakdown is one of the most obvious OA indicators, it is also possible to determine bone cysts, osteophytes, and deformation of the bone ends. In addition to the X-ray examination, a sample of synovial fluid can be withdrawn from the joint cavity and examined in terms of component concentrations and physical features like viscosity and pH.

In order to classify the severity of an OA condition, grades from 0 (healthy) to 4 (severe) were introduced. Radiographic as well as laboratory and clinical examination results are consulted to determine such a grade (Flores and Hochberg, 2003).

OA is not yet curable; the applied treatment is mostly symptomatic. For the patient it is especially the pain that causes difficulty in managing everyday life. For this reason the major treatment options refer to analgesics and physiotherapy. In severe cases of OA, a joint replacement can be necessary (Ross, 1997). In order to be able to cure or even prevent the disease, it is important to investigate and understand the cellular and molecular background of OA.

2.2 Osteoclastogenesis and the Importance of RANKL

For a long time the skeleton was considered to be a rather static component of the body and once built, hardly remodelled over a lifetime. During the last twenty years however, remarkable progress has been made concerning the molecular and cellular features of bone and cartilage development (Karsenty and Wagner, 2002).

There are two fundamentally important cell types that control the lifetime of bone tissue: osteoblasts, which are responsible for bone formation and their counterparts, the bone resorbing osteoclasts. These cells form a dynamic equilibrium and work to maintain the total bone mass at a constant level.

Osteoblasts are mononucleate cells of mesenchymal origin and are often referred to as sophisticated fibroblasts, as they show almost the same gene expression pattern. Activated osteoblasts produce osteoid, a precursor of the mineralised bone matrix. During this process, the cells can get embedded into the bone tissue and eventually differentiate into osteocytes (Karsenty, 1999).

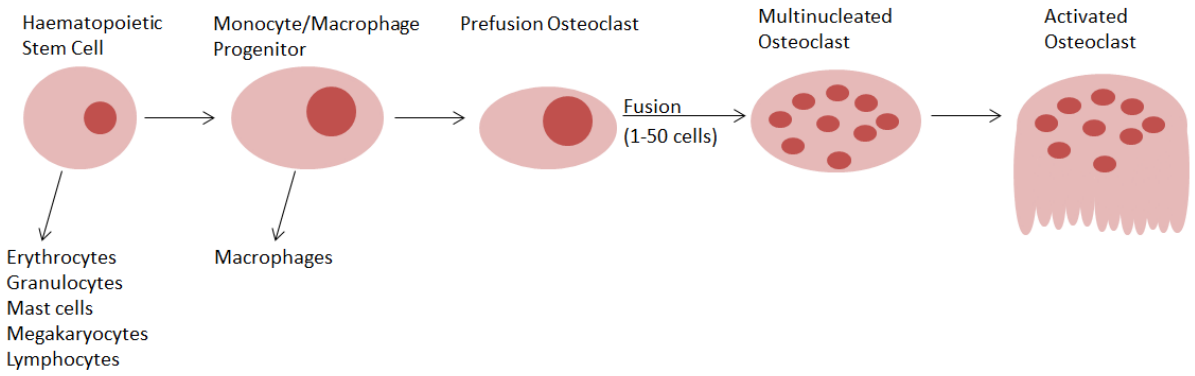

Figure 2 Osteoclast differentiation from hematopoietic stem cells. The fully differentiated and functioning osteoclast is a multinucleated cell with ruffled borders.
Based on: Karsenty and Wagner, 2002 Figure 5

Osteoclasts possess 1-50 nuclei, depending on the species, and derive from haematopoietic stem cells. Another main characteristic is their ability for tartrate-resistant acid phosphatase (TRAP) staining. Their development from stem cells to fully differentiated and functional osteoclasts is illustrated in Figure 2.

The process begins with the multipotent haematopoietic stem cell that can evolve into every kind of myeloid and lymphoid blood cell. After developing into a monocyte/macrophage progenitor cell, it can differentiate into a progenitor osteoclast. The fusion of up to 50 cells results in a multinucleated osteoclast that in turn gains its function by activation. Phenotypically, a mature and activated osteoclast can be identified by its multinucleation and the ruffled border as shown in Figure 2.

Osteoclast differentiation and activation takes place under the influence of numerous transcription factors and signalling molecules, many of them not fully identified yet (Karsenty and Wagner, 2002). For this reason and to allow a better understanding, the following description will be simplified to only a few important molecules that contribute to osteoclastogenesis: macrophage colony-stimulating factor (M-CSF), receptor activator of nuclear factor κ B (RANK), its ligand (RANKL), as well as the associated transcription factors nuclear factor κ B (NFκB), and nuclear factor of activated T-cells, cytoplasmic 1 (NFATc1).

M-CSF is a secreted cytokine that is essential for the maturation of macrophages; its receptor c-Fms is also found on the cell surface of osteoclast precursors, which gives reason to the presumption that M-CSF plays an important role in osteoclastogenesis (Karsenty and Wagner, 2002). As a matter of fact, it has been found that mice with inactivated *M-CSF* genes possess neither mature macrophages nor osteoclasts. As a result, they suffer from osteopetrosis, a

disease that causes increased bone density, and can be healed by application of M-CSF (Kodama et al., 1991).

RANKL was discovered by first identifying its inhibitor osteoprotegerin (OPG), which is secreted by osteoblasts. As overexpression of OPG leads to osteopetrosis in murine models (Simonet et al., 1997), it was presumed that this molecule plays a role in the osteoblast/osteoclast homoeostasis; RANKL was eventually determined to be the molecule inhibited by OPG. RANKL belongs to the family of TNF and occurs in either membrane-bound or soluble states. It is particularly found in bone and bone marrow, especially on the surface of preosteoblasts, but it is also expressed in lymphoid tissues, where it has several effects on immune cells (Khosla, 2001; Xing et al., 2005). In addition to its important role in osteoclastogenesis, RANKL is involved in communication processes between T-cells and dendritic cells (Anderson et al., 1997); hence, T-cells have the ability to express *RANKL*. *In vitro*, stimulation with the antibody anti-CD3 is necessary to mediate a measureable expression of *RANKL* in murine T-cells (Josien et al., 1999; Wang et al., 2002), which was also found to be true for human T-cells during this work. Soluble RANKL has a molecular weight of approximately 31 kDa and is derived by cleavage of the membrane-bound form (Khosla, 2001); the gene sequence consists of 546 bp and can be found in chapter 4.1.

The RANKL receptor RANK was found to be produced particularly by both osteoclast precursor cells and mature osteoclasts (Hsu et al., 1999), as well as by dendritic cells. However, unlike RANKL, it has not been discovered on the cell surface of other body cells (Xing et al., 2005). The interaction of RANKL with its receptor RANK on the cell surface of osteoclasts triggers signalling pathways that are involved in osteoclast differentiation, fusion, activation, and survival (Khosla, 2001)

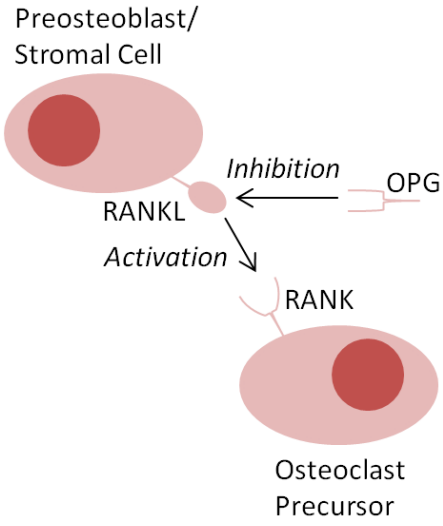

Figure 3 Interactions between OPG, RANKL, and RANK. OPG inhibits RANKL, whereas RANKL activates RANK on the surface of osteoclast precursor cells.
Based on: Khosla, 2001 Figure 1

The close relationship between OPG, RANKL, and RANK is summarised in Figure 3. The receptor RANK on the surface of osteoclasts is activated by its ligand. RANKL in turn can be inhibited by its decoy receptor OPG. The balance between activation of RANK and inhibition of RANKL controls the dynamic process of bone resorption. *In vivo*, the cell-cell interactions between osteoclasts and osteoblasts lead to the formation of active osteoclasts. Thus, the development of osteoclasts is controlled by their counterparts, the osteoblasts, and the sensitive interplay of bone breakdown and formation is held in balance.

Before RANKL and its receptor RANK were determined, osteoclasts needed to be generated in co-cultures with osteoblasts. As the most important factors contributing to osteoclast differentiation are now known, it is possible to generate mature, active osteoclasts by adding M-CSF and soluble RANKL to a culture of osteoclast precursor cells (Khosla, 2001).

Both M-CSF and RANKL bind to their receptors on the osteoclast precursor surface, thereby provoking signalling cascades that ultimately lead to the activation of numerous transcription factors and consequently to the differentiation into osteoclasts. One such transcription factor activated by RANK is NFκB, which is a protein complex that is involved in many signalling

pathways concerning cell differentiation; it occurs in a variety of different cell types and research suggests that it plays a decisive role in osteoclastogenesis. Two of the NFκB subunits, p50 and p52, have been found to be most crucial in the early phases of differentiation. Mice lacking both of the subunits were osteopetrotic due to missing osteoclasts, however, mice with only one of these subunits not expressed had phenotypically unaltered bones (Soysa and Alles, 2009).

NFATc1 has been determined as the key transcription factor in osteoclastogenesis. The family members of the NFAT transcription factors are activated by the phosphatase calcineurin, which is dependent on the intracellular calcium concentration. Hence, NFATc1 is regulated by the calcium concentration inside the cell; it is also induced by NFκB and another transcription factor named activator protein 1 (AP-1) (Takayanagi, 2007).

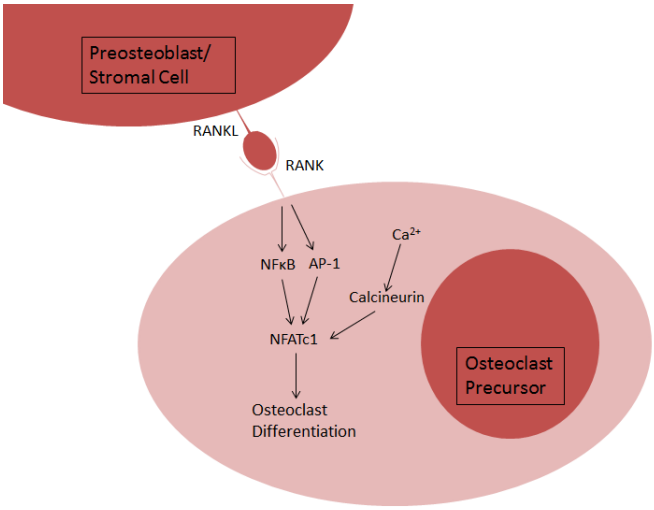

Figure 4 Signaling cascades in osteoclastogenesis. The activation of RANK by its ligand RANKL induces the activation of transcription factors such as NFκB and AP-1. These transcription factors together with calcineurin activate the key transcription factor NFATc1.
Based on: Takayanagi, H. 2007 Figure 1

The signalling cascade is summarised in Figure 4. The interaction between RANK and its ligand leads to the activation of several transcription factors, such as NFκB and AP-1. Together with the calcium-dependent phosphatase calcineurin, they activate NFATc1, the key transcription factor in osteoclastogenesis.

2.3 The Role of Osteoclasts in Osteoarthritis

In chapter 2.2, it was shown that there is a well-balanced equilibrium between bone breakdown by osteoclasts and the formation of new bone tissue by osteoblasts. This process is constantly taking place in healthy bones, and is called bone remodelling or bone turnover. A disturbance in this homoeostasis can lead to diseases such as OA, osteoporosis, osteopetrosis, and a number of relatively rare bone diseases (Karsenty, 1999).

In terms of OA, it has been shown that there is indeed an increased bone turnover. In animal models, a loss of subchondral bone in early stages of OA has been detected, followed by an increase in bone formation in later stages that subsequently led to the development of osteophytes and skeletal sclerosis, i.e., increased and inhomogeneous bone density (Hayami et al., 2004). This pathological condition indicates that there is a decline in either osteoclast number or osteoclast function, resulting in disproportionate bone formation compared to bone resorption.

It has been shown that the most characteristic attribute of osteoarthritic joints, namely cartilage degradation, is closely linked to the occurrence of sclerotic subchondral bone. It has even been suggested that the cartilage degrading chondroclasts should be reclassified as another type of osteoclasts, resorbing cartilage instead of bone (Henriksen et al., 2011). In this case, two entirely different types of osteoclast dysfunctions would contribute to OA: overexpression in terms of articular cartilage breakdown, and a lack of function leading to alterations in the subchondral bone.

It has become clear in recent years that OA is far more complex than just the age-related ′wear and tear′ of cartilage; conversely, there are genetic as well as environmental factors contributing to the disease. Furthermore, the immune system is thought to have a far more

important influence than previously assumed (Ferrell et al., 2003). However, the exact role of osteoclasts in outbreak and development of OA remains to be determined.

Such an investigation should be based on first finding out about the function of healthy osteoclasts and subsequently studying the different compounds and their interactions with each other and how they contribute to osteoclast differentiation and function. It is probable that it is one or several of these components that, when not working properly, contribute to OA.

2.4 The Flp-In™ System and the pSecTag/FRT/V5-His-TOPO® TA Expression Kit

Most of the used methods for this work are basic procedures in molecular biological practice and do not require detailed explanation. The expression kit that was used for this work however is briefly described in order to provide a better understanding of the various steps that were undertaken, whereas the exact procedural methods are explained in chapter 3.

The Flp-In™ System combines the Flp recombinase and the Flp Recombination Target (FRT) from the yeast *Saccharomyces cerevisiae*, where they are located on a self-replicating plasmid named 2 µM circle. FRT consists of a repetitive sequence and acts as a binding site for Flp recombinase, which cleaves one strand of the FRT site. By cleaving two FRT sites, a Holliday junction is formed that eventually disintegrates into two recombinant double strands (Zhu and Sadowski, 1995). By equipping both, the genomic DNA of the host cell and the plasmid that contains the gene of interest, with an FRT site and by inserting another plasmid that contains the genetic information for Flp recombinase, it is possible to integrate the extrachromosomal DNA in the host genome.

The vector pSecTag/FRT/V5-His-TOPO® is 5185 bp long; a linear display with the most essential features and their positions in the vector (in bp) is shown in Figure 5.

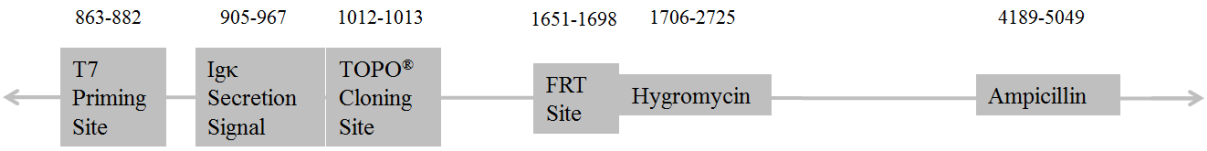

Figure 5 pSecTag/FRT/V5-His-TOPO® vector in linear display with the most essential components and their positions (in bp).
Based on: Invitrogen, 2010 p. 27

The T7 priming site allows sequencing of the insert it also acts as a promotor region that enables transcription of the gene of interest. The murine Ig κ-chain secretion signal is expressed as a fusion protein together with the cloned gene. It enables the secreted expression of the gene of interest, which simplifies harvesting the product. The TOPO® cloning site contains single thymidine overhangs at its 3′ ends. By using a polymerase that adds adenine overhangs at the 5′ ends of a gene during amplification, a DNA sequence is generated that can ligate naturally with the vector. Topoisomerase, an enzyme that is attached to the cloning site, catalyses the ligation of vector and insert. The Flp Recombination Target (FRT) site is a binding site for Flp recombinase and enables integration of the plasmid in the genome as previously described. Two antibiotic resistance genes on the plasmid allow bacterial and mammalian cell selection. Successfully transformed bacteria are resistant against ampicillin and transfected mammalian cells express a hygromycin resistance gene.

3. General Material and Methods

3.1 Cell Cultures

Two different cell lines were routinely cultured for this work: Jurkat cells, a cell line of immortal T lymphocytes that was established in the 1970s (Schneider et al., 1977), and CHO cells, the most commonly used eukaryotic cells for the production of recombinant proteins (Kim et al., 2012).

3.1.1 Jurkat Cells

Jurkat cells (ECACC, cat# 88042803) were routinely cultured in tissue culture flasks using RPMI 1640 medium (Life Technologies, cat# 21875-034) supplemented with 10 % (v/v) foetal bovine serum (FBS) (Life Technologies, cat# 10437-028), 2 mM L-glutamine (Life Technologies, cat# 25030-024), 100 U mL^{-1} penicillin, and 100 µg mL^{-1} streptomycin (both Life Technologies, cat# 15070-063). The cells were constantly kept in a humidified incubator at 37 °C, 5 % CO_2 concentration and medium was changed when the cell solution had adopted a yellow/orange colour due to pH changes. PBS (Life Technologies, cat# 14200-067) was used for washing the cells.

For *RANKL* expression, medium was supplemented with the antibody anti-CD3 (obtained from Prof. Doreen Cantrell, University of Dundee) and the cells were cultured under these conditions for 48 h. For experimentation concerning *RANKL* expression in Jurkat cells, the antibody anti-CD28 (Doreen Cantrell, University of Dundee) was used.

3.1.2 CHO Flp-In Cells

CHO Flp-In cells (Life Technologies, cat# R758-07) were routinely cultured in tissue culture flasks using F-12 + GlutaMAX^{TM}-I Nutrient Mixture (Life Technologies, cat# 31765-027) supplemented with 10 % (v/v) FBS (Life Technologies, cat# 10437-028), 2 mM L-glutamine (Life Technologies, cat# 25030-024), 100 U mL^{-1} penicillin, and 100 µg mL^{-1} streptomycin

(both Life Technologies, cat# 15070-063). The cells were constantly kept in a humidified incubator at 37 °C, 5 % CO_2 concentration and passaged at 70-80 % confluence, using trypsin-EDTA solution (Sigma, cat# T4049) for trypsinising and PBS (Life Technologies, cat# 14200-067) for washing the cells.

3.1.3 Further Cell Lines

The monocytic cell lines AML3 and HL60, the B lymphocytes PGA, HG3, and B4, as well as the T lymphocytes CEM, HUT, Jurkat, and Jurkat that had been stimulated with the antibodies anti-CD3 (1.1 µg mL^{-1}) and anti-CD28 (0.5 µg mL^{-1}) for 48 h are leukaemic cell lines that were not cultivated for this work, but currently existing RNA samples were used to examine whether or not *RANKL* is expressed in these cell lines.

3.2 Gene Amplification and Gene Expression Analysis

In order to obtain amplified genes three steps were routinely conducted; total RNA was extracted from cell cultures, transcribed into complementary DNA (cDNA) via reverse transcription (RT), and the gene of interest was amplified using polymerase chain reaction (PCR). In case of the previously acquired RNA samples of cell lines that mentioned above, only RT and PCR were conducted.

3.2.1 RNA Extraction and Quantification

Cells were stained with Trypan Blue Solution (Sigma, cat# T8154) and counted using a haemocytometer (Neubauer); total RNA was extracted from up to 10^7 cells using the GeneJET RNA Purification Kit (Thermo Scientific, cat# K0731). The resulting RNA concentration was measured in 2 µL sample volume at a wavelength of 260 nm using the NanoDrop® Spectrophotometer ND-1000 (NanoDrop); RNA samples were then stored at −20 °C prior to further use.

3.2.2 Reverse Transcription

RNA was converted to cDNA using the MyCycler™ Thermal Cycler (Bio-Rad) and a protocol consisting of 1 stage at 25 °C for 10 min, 1 stage at 37 °C for 120 min, and 1 stage at 85 °C for 5 min.

RT was performed at standard conditions that incorporated 0.04 µg µL^{-1} total RNA, 0.1 U µL^{-1} Affinity Script™ Multiple Temperature Reverse Transcriptase (Agilent Technologies, cat# 600109-51), 0.1 µL µL^{-1} 10x Affinity Script™ Multiple Temperature Reverse Transcriptase Buffer (Agilent Technologies, cat# 600100-51), 0.04 µL µL^{-1} 10x Random Primers (Applied Biosystems, cat# 4319979), 0.8 mM dNTP (Applied Biosystems, cat# AM8200), 0.8 U µL^{-1} RNase Inhibitor (Applied Biosystems, cat# N808-0119). When formation of secondary RNA structures needed to be inhibited, the reaction mix additionally contained 60 mM DTT (Sigma, cat# 43816). In conjunction with the RNA samples, a negative control sample consisting only of molecular biology grade water (from laboratory stock) was prepared to check for genomic contaminations.

3.2.3 Polymerase Chain Reaction

For PCR amplification of *RANKL*, either the MyCycler™ Thermal Cycler or the MJ Mini™ Personal Thermal Cycler (both Bio-Rad) was used. The protocol consisted of 1 stage at 95 °C for 2 min, 35-40 cycles of 95 °C for 40 s (denaturation), 60 °C for 30 s (primer annealing), and 72 °C for 60 s (elongation), and 1 stage at 72 °C for 7 min.

The reaction mix was made up of 0.02 U µL^{-1} GoTaq® DNA Polymerase (Promega, cat# M830B), 0.2 µL µL^{-1} 5x Green GoTaq® Flexi Buffer (Promega, cat# M891A), 0.08 mM dNTP (Applied Biosystems, cat# AM8200), 2.5 mM $MgCl_2$ (Promega, cat# A351H) and 0.2 pmol µL^{-1} 5′ as well as 3′ Primers (Eurofins MWG Operon, design by Dr. Robin Freeburn). *RANKL* primers were designed with a predicted melting temperature of

approximately 65 °C and, when possible, included an intron:exon boundary. The following primer pair was used for *RANKL* amplification:

Forward, 5′-GAG AAA AGC GAT GGT GGA TGG C-3′

Reverse, 3′ CAC TCC AAA AAC TGG GGC TCA 5′

When the PCR product was meant to be cloned into a plasmid, the reaction mix contained 0.03 U μL^{-1} Easy-A Hi-Fi PCR Cloning Enzyme (Agilent Technologies, cat# 600400-51), 0.1 µL µL 10x Easy-A Reaction Buffer (Agilent Technologies, cat# 600400-52) and no additional $MgCl_2$.

When samples were to be analysed by gel electrophoresis, PCR products were merged with 20 % (v/v) Blue/Orange 6x Loading Dye (Promega, cat# G190A) and then separated on ethidium bromide (Sigma, cat# E1510) 1 % agarose gels (Severn Biotech, cat# 30-10-10) using tris/borate/EDTA running buffer (Sigma, cat# T4415). For size evaluation, two lanes of HyperLadder I (Bioline, cat# BIO-33053) were additionally loaded onto the gel.

3.2.4 Quantitative Real-Time PCR

Quantitative Real-Time PCR (qRT-PCR) is a technique that allows amplification and simultaneous quantification of a gene by coupling the elongation process with a fluorescent signal; the number of cycles that it takes to obtain a measurable fluorescence is called threshold cycle (C_T) and is used in the calculation of the relative gene expression compared to an endogenous control gene and a calibrator sample (Logan et al., 2009). The StepOnePlus™ Real-Time PCR System (Applied Biosystems) and the corresponding Fast SYBR® Green Master Mix (Applied Biosystems, cat# 4385612) were used for qRT-PCR. The used protocol consisted of 1 stage at 95 °C for 20 s, followed by 40 cycles of 95 °C for 5 s (denaturation), and 60 °C for 60 s (primer annealing and elongation). After the amplification, a melt curve was plotted by implementing 1 stage at 95 °C for 15 s, 1 stage at 60 °C for 90 s, 1 stage in

which the temperature increased gradually, and 1 stage at 95 °C for 15 s. For the quantification of target genes a primer pair for the housekeeping gene *RNF20* (Eurofins MWG Operon, design by Dr. Robin Freeburn) was used as an endogenous control.

3.3 Cloning

For cloning and expression of *RANKL*, the pSecTag/FRT/V5-His TOPO® TA Expression Kit (Life Technologies, cat# K6025-01) was used. All procedures were performed according to the manual (Life Technologies, 2010) if not indicated otherwise.

3.3.1 Cloning, Transformation and Plasmid Extraction

The PCR product containing *RANKL* was cloned into the expression vector and then transformed via One Shot® chemical transformation into chemically competent *E. coli* MAX Efficiency® DH5α™ (Life Technologies, cat# 18258-012). Cell suspensions were spread on petri dishes containing nutrient agar (LAB M, cat# LAB008) on which 100 µL of 50 µg mL^{-1} ampicillin (Life Technologies, cat# 11593-027) was spread and grown overnight at 37 °C. From each petri dish five colonies were picked and grown in 5 mL of Luria-Bertani (LB) medium (LAB M, cat# LAB169) supplemented with 100 µg mL^{-1} ampicillin (Life Technologies, cat# 11593-027), and grown for 24 h in a shaking incubator at 37 °C and a revolution speed of 120 rpm.

Plasmids from these cultures were extracted using an alkaline lysis plasmid miniprep (Ausubel et al., 1999). Solution I is made up of 50 mM glucose (Sigma, cat# G8270), 25 mM tris-HCl (Boehringer Mannheim, cat# 812846), and 10 mM EDTA (Sigma, cat# E5134). Solution II is made up of 200 mM NaOH (Fisher Scientific, cat# 1310-73-2), and 10 g L^{-1} SDS (Sigma, cat# L4390). Solution III is made up of 294 g L^{-1} potassium acetate (VWR, cat# 26664.293), and 115 mL L^{-1} glacial acetic acid (Sigma, cat# A6283). Furthermore, phenol:chloroform:isoamyl alcohol (Sigma, cat# P3803) and ethanol (Fisher Scientific, cat# UN1170) were used for plasmid precipitating and washing.

Obtained plasmids were analysed for presence and orientation of the inserted gene; a common method is digestion with restriction enzymes and subsequent analysis of the resulting fragments by electrophoresis. For this work however, a PCR based method was developed, whereby a plasmid sequencing primer was used as forward primer combined with either the *RANKL* reverse or forward primer used as reverse primer. In the case of correct orientation, the combination with *RANKL* reverse resulted in a band of approximately 700 bp, whereas no band could be seen when combined with *RANKL* forward. A reversely inserted gene resulted in the reciprocal pattern.

Samples with correctly inserted gene were sent for sequencing to GATC Biotech Ltd. (London) in order to check for mutations that may have occurred during PCR.

Clones that proved to be successfully transformed were grown in 75 mL LB medium (LAB M, cat# LAB169) supplemented with 50 µg mL^{-1} ampicillin (Life Technologies, cat# 11593-027) and grown for 16 h in a shaking incubator at 37 °C and a revolution speed of 150 rpm.

Plasmids from these cultures were meant for transfection into CHO Flp-In cells and were extracted using the Qiagen® Plasmid Midi Kit (25) (Qiagen®, cat# 12143) as well as isopropanol (Sigma, cat# I9516). Extracted plasmids were sterilized by washing with 100 % ethanol (Fisher Scientific, cat# UN1170) and stored in sterile molecular biology grade water (from laboratory stock) at 4 °C prior to transfection.

3.3.2 Transfection

CHO cells were transfected with the obtained plasmid by lipofection, a technique that includes the formation of liposome DNA complexes and intake of the plasmid through endocytosis (Felgner et al., 1987). Oligofectamine™ Reagent (Life Technologies, cat# 12252-011), and PLUS™ Reagent (Life Technologies, cat# 11514-015) were used for

lipofection; cells were split 1:10 the day after transfection. For selection of successfully transfected CHO cells with the *RANKL* containing plasmid, 500 µg mL^{-1} of the antibiotic hygromycin B (EMD Millipore, cat# 400051) was added to the medium two days after transfection. Selection took place for three weeks, changing the selective medium every three days. Two negative control cultures that had not been transfected were treated in the same manner. Selection was considered completed, when no surviving cells were left in the negative control culture.

3.4 Protein Analysis

Protein analysis was conducted using the 2100 Bioanalyzer (Agilent Technologies) and the corresponding Agilent High Sensitivity Protein 250 Kit (Agilent Technologies, cat# 5067-1575). This method comprises two steps: in a first reaction, ε-amino groups of lysine amino acids in the protein are labelled with a fluorescent dye, proteins are then separated on a chip according to the principles of gel electrophoresis and detected by their fluorescent labelling.

Supernatants of transfected CHO Flp-In cells were analysed by this method for the presence of RANKL, while a supernatant of untransfected CHO Flp-In cells served as negative control and the same supernatant spiked with 50 µM RANKL (Peprotech, cat# 310-01) as positive control; all samples were analysed in duplicate. Due to difficulties concerning determination of RANKL, the protein IFN-α (obtained from Gartnavel General Hospital, Glasgow) was additionally analysed.

All samples were examined using three different sample preparation methods: centrifugation to dispose of dead cells, centrifugation and following acetone precipitation (Fisher Chemical, cat# A/0560/PC21), and centrifugation with following precipitation of RANKL using the Immunoprecipitation Kit – Dynabeads® Protein G (Life Technologies, cat# 100.07D) and RANKL antibody (N-19) (Santa Cruz Biotechnology, cat# sc-7628). The latter is based on a

principle combining magnetic beads bound to Protein G and a specific antibody, in this case anti-RANKL. The antigen binds to its specific antibody, the antibody in turn binds to Protein G, which is bound to a magnetic bead; using a magnet, the protein-antibody-complex can easily be separated from other proteins in the sample. According to a protocol developed by Agilent Technologies, the method consists of labelling with the fluorescent dye, immunoprecipitation, and subsequent analysis using the 2100 Bioanalyzer (Wenz and Rüfer, 2010).

4. Experimental Results

The first consideration was to amplify the gene *RANKL*, using total RNA from different T-cell lines as a template. The resulting PCR product was then cloned into an expression vector. After transforming *E. coli* with this plasmid, analysis of insert orientation and sequence was used to select a clone that possessed a plasmid with correctly inserted and not mutated *RANKL*. The plasmid was purified and transfected into CHO Flp-In cells that then expressed *RANKL* and secreted the protein.

4.1 Screening for *RANKL* Expression in Leukaemic Cell Lines

As previously discussed, *RANKL* was found to be expressed particularly by bone, bone marrow and lymphoid cells (Khosla, 2001). For this reason, a screen was conducted, examining total RNA samples by qRT-PCR from a selection of leukaemic cell lines. The cell lines AML3, HUT, CEM, HG3, HL60, PGA, B4, Jurkat and Jurkat that had been stimulated with anti-CD3 and anti-CD28 for 48 h (aCD3/aCD28) were chosen for this examination. The qRT-PCR software automatically calculates a C_T value for each primer set and gene, which can then be used to calculate the relative gene expression (RQ) of a sample compared to a control sample (calibrator). When C_T values for an endogenous control or housekeeping gene ($C_{T,HK}$) and a calibrator ($C_{T,C}$) are available, the relative gene expression can be calculated by

$$\mathrm{RQ} = 2^{-\Delta\Delta C_T}$$

with

$$\Delta\Delta C_T = \Delta C_T - C_{T,C}$$

and

$$\Delta C_T = C_T - C_{T,HK}$$

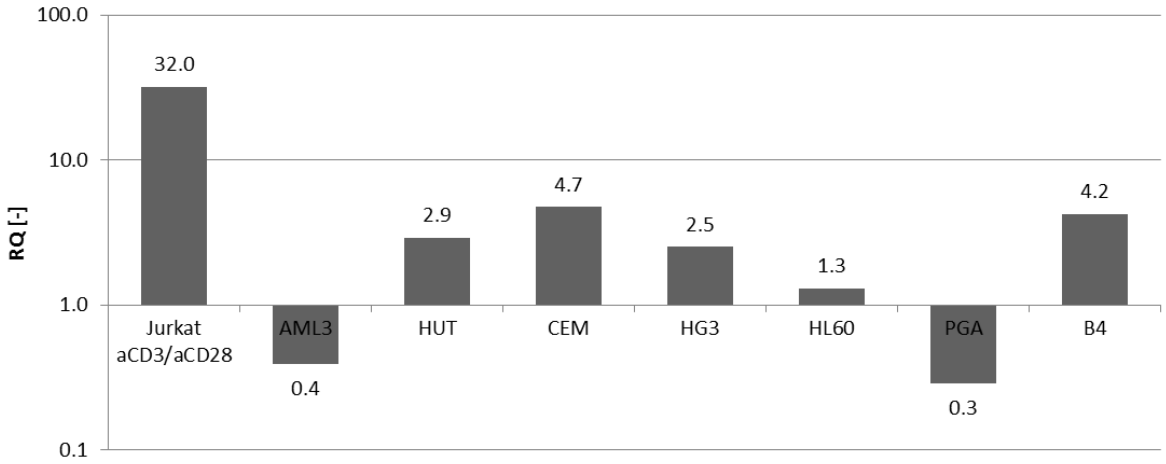

Figure 6 Relative *RANKL* expression of different leukaemic cell lines. RQ was calculated by using expression of the housekeeping gene *RNF20* as endogenous control and *RANKL* expression in unstimulated Jurkat cells as a calibrator.

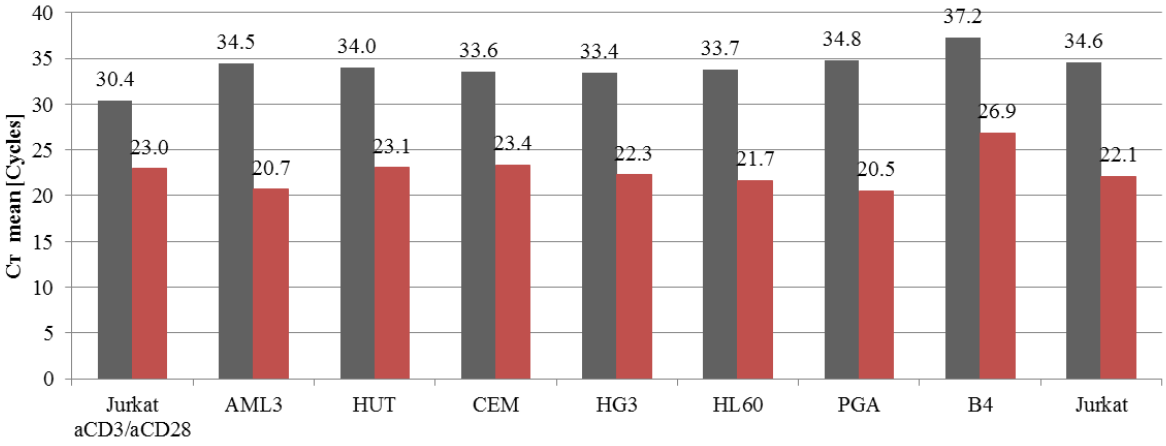

Figure 7 Average C_T values resulting from qRT-PCR reactions amplifying *RANKL* (grey) and the housekeeping gene *RNF20* (red) in leukaemic cell lines.

Figure 6 summarises the result of the first screening; the amplification of the housekeeping gene *RNF20* was used as endogenous control, C_T values of *RANKL* amplification in unstimulated Jurkat cells were used as a calibrator, as T-cells, like Jurkat, are known to express *RANKL in vivo* (Wong, et al., 1997). According to Figure 6, the cell lines AML3 and PGA do not express noticeably high levels of *RANKL*, their *RANKL* expression levels are only 40 % and 30 % of the expression level in unstimulated Jurkat cells, respectively. The expression levels in the cell lines HUT, CEM, HG3, HL60, and B4 are not significantly higher than in unstimulated Jurkat cells. However, judging from the amplification plots and average C_T values shown in Figure 7, none of these cell lines, including the calibrator Jurkat, featured a significantly high level of *RANKL* expression (shown in grey) compared to *RNF20*

expression (red). Whilst amplification of *RNF20* led to C_T values between 20 and 24 cycles in all samples, except B4, which was marginally higher, the C_T values for *RANKL* are all above 33 cycles, which usually indicates that amplification was not successful. Interestingly, the stimulated Jurkat cells showed promising results; as shown in Figure 6, *RANKL* expression in these cells was more than 30-fold higher than for their unstimulated equivalents. Furthermore, as is shown in Figure 7, Jurkat aCD3/aCD28 were the only cells that achieved a ΔC_T of less than 10 cycles (with C_T = 30.4 cycles for *RANKL* and 23.0 for *RNF20*). The fact that these samples only differed following stimulation with anti-CD3 and anti-CD28 led to the idea to set up a time course in which Jurkat cells were stimulated with both antibodies over a period of 72 h, with RNA samples for RT and qRT-PCR being taken every 24 h. The PCR was repeated under the same conditions, using *RNF20* and *RANKL* expression in unstimulated Jurkat cells (t = 0) as endogenous control and calibrator, respectively. The relative *RANKL* expression plotted over the stimulation time is shown in Figure 8; however, the curve consists of only the four data points t = 0, t = 24 h, t = 48 h, and t = 72 h, and it is therefore difficult to draw exact conclusions with respect to *RANKL* expression.

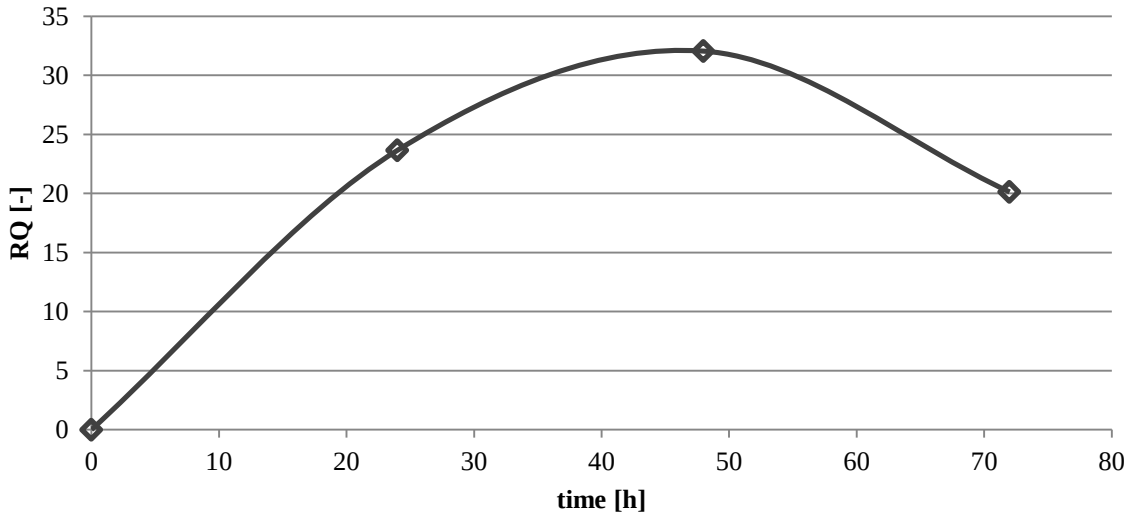

Figure 8 Relative *RANKL* expression in Jurkat cells that have been stimulated with anti-CD3 and anti-CD28 plotted over time. *RNF20* was used as endogenous control and *RANKL* expression at time t = 0 as a calibrator.

According to Figure 8, *RANKL* expression increases with stimulation time, reaching a maximum after 48 h and decreasing afterwards. These results should be considered tentatively because of the limited number of data points, as it is possible that an error in sample preparation or procedural method occurred, which would have particular implications for the last data point. For this reason, a duplicate experiment was conducted, whereby another culture of stimulated Jurkat cells was prepared, using the same antibody concentrations. For this experiment, samples were withdrawn after 24 h, 48 h, 70 h, and 96 h, and *RANKL* was amplified via standard PCR using GoTaq polymerase, the PCR products were separated by gel electrophoresis. A very diffuse and weak band at approximately 550 bp was observed in the t = 48 h sample, but in none of the other samples (data not shown), confirming the previous findings that *RANKL* expression is at its maximum after 48 h of stimulation with anti-CD3 and anti-CD28. Any further purification of the PCR product by cutting out the band, melting it and using it as a template for another PCR did not lead to a sharper band. The fact that it was not possible to amplify greater amounts of *RANKL* led to the conclusion that the used primer pair was not able to anneal optimally to the single stranded DNA during PCR. For this reason, another 5′ primer (5′b) and two further 3′ primers (3′b and 3′c) were designed, which are shown together with the original primers 5′a and 3′a in Table 1 and Figure 9.

Table 1 5′ and 3′ *RANKL* primers that were used for amplification by qRT-PCR of *RANKL* in total RNA samples of different cell lines.

Primer	Sequence
5′a	5′ GAG AAA GCG ATG GTG GAT GG 3′
5′b	5′ GAG AAA GCG ATG GTG GAT GGC 3′
3′a	3′ GGG GCT CAA TCT ATA TCT C 5′
3′b	3′ GGC TCA ATC TAT ATC TCG AAC 5′
3′c	3′ CAC TCC AAA AAC TGG GGC TCA 5′

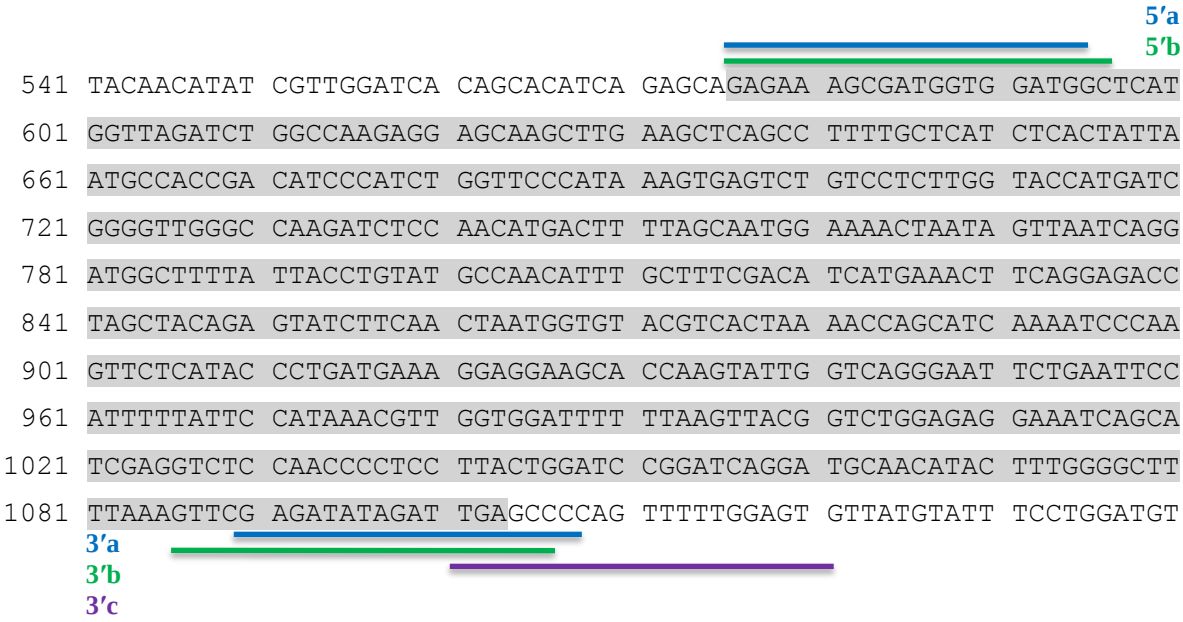

Figure 9 Position 541 to 1140 (in bp) of *RANKL*. The part encoding for the soluble protein domain is highlighted grey, the annealing positions of the different 5′ and 3′ primers are shown as colored lines.

The choice of the 5′ primer was limited, as only the part of the gene encoding for the soluble part of the protein (highlighted grey in Figure 9) was to be amplified. Accordingly, the two 5′ primers only differed by one base pair and were less likely to cause noticeable differences in terms of annealing ability. The coding region of the gene ends with the stop codon (TGA), which meant it was possible to design a broader variety of 3′ primers, as long as they incorporated this stop codon. All possible primer combinations were used in qRT-PCR reactions on the 48 h stimulation sample.

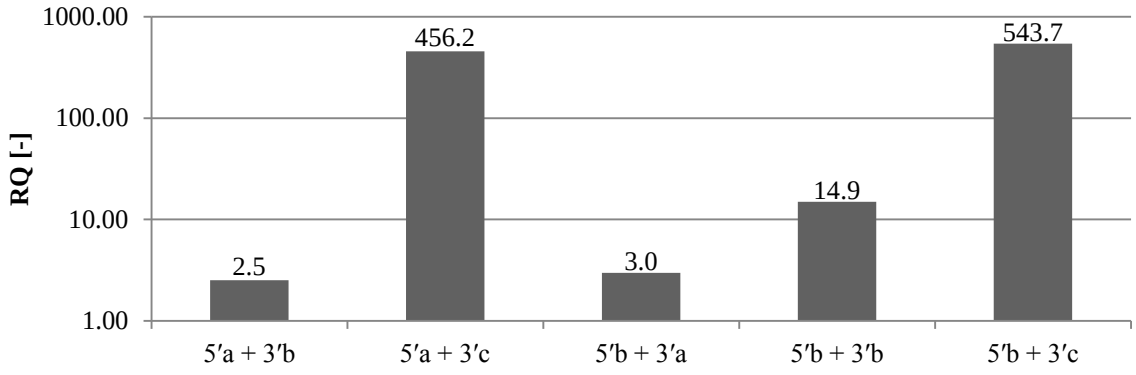

Figure 10 Relative *RANKL* expression in Jurkat cells that were stimulated with anti-CD3 and anti-CD28 for 48 h using different combinations of *RANKL* 5′ and 3′ primers for qRT-PCR. Amplification with the original primer pair 5′a + 3′a served as calibrator, expression of *RNF20* as endogenous control.

Figure 10 shows the relative *RANKL* expression in the same sample with different primer combinations, using *RNF20* as endogenous control and the C_T value from the amplification with the original primer pair (5′a + 3′a) as a calibrator. Interestingly, primer combinations with the 3′c primer show noticeably higher RQ values; using these primer pairs, the relative *RANKL* expression appears to be more than 400-fold higher than with primer combinations using the 3′a or 3′b primer.

Figure 11 displays an amplification plot (fluorescent signal ΔRn is plotted logarithmically against the number of cycles) using the two *RANKL* primer pairs 5′b + 3′c (red) and 5′a + 3′a (blue). In addition, *RNF20* (purple) in the same sample was amplified, and a water sample amplified with *RNF20* primers served as a negative control (green).

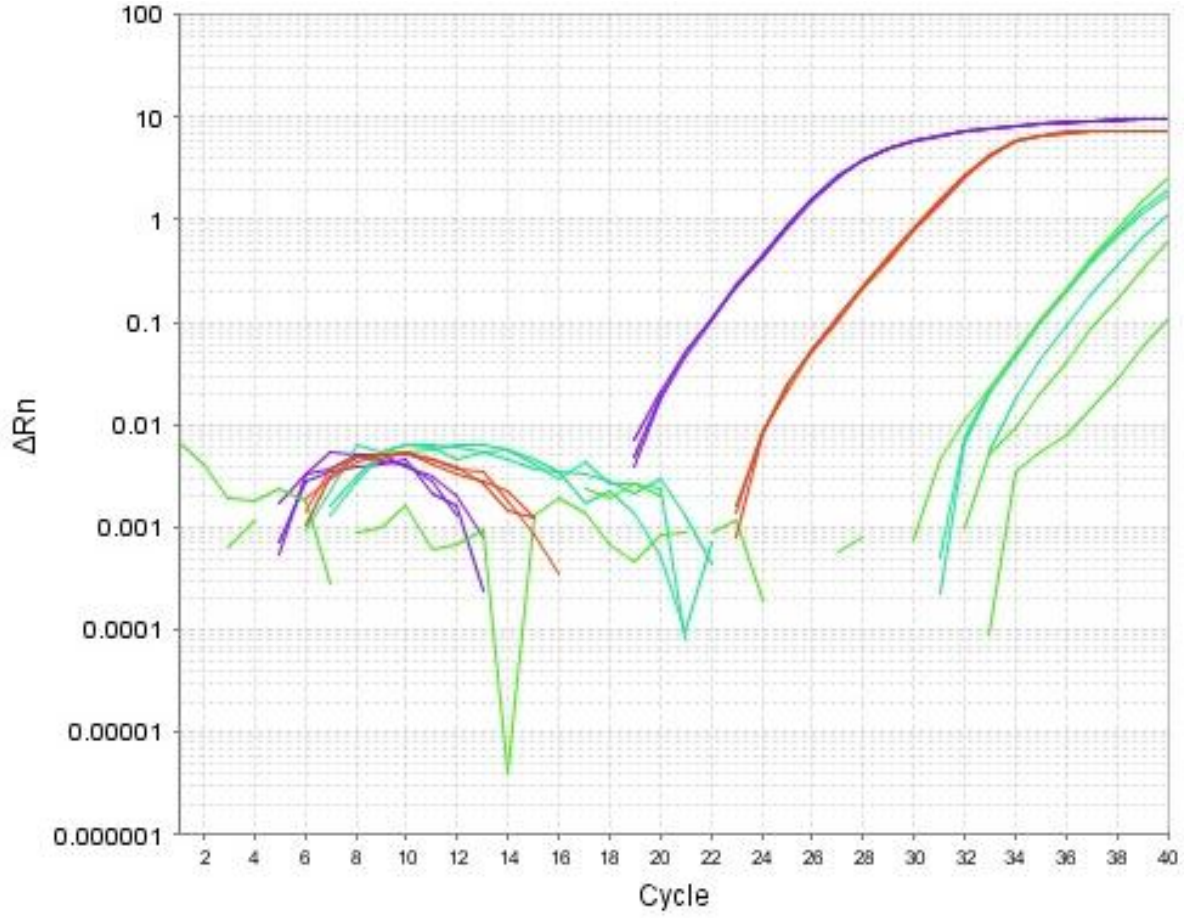

Figure 11 Amplification plot of an RNA sample of Jurkat aCD3/aCD28 cells using two different *RANKL* primer pairs: 5′b + 3′c (red) and 5′a + 3′a (blue) in comparison to amplification of the housekeeping gene *RNF20* (purple) and a negative control (Water, green).

Comparing the amplification plots of both *RANKL* primer pairs and considering the immense differences in RQ values shown in Figure 10, it becomes obvious how crucial the choice of a suitable primer pair is, given that the exact same sample was used in both cases. In this sample, the average C_T for amplification of *RNF20* is 20.5 cycles. For the primer pair 5′b + 3′c the fluorescent signal reaches the threshold after 26.7 cycles, whereas the amplification plot with primer pair 5′a + 3′a with an average C_T of 34.9 cycles is barely distinguishable from the negative control sample, which showed an average C_T of 36.5 cycles. These results demonstrate how amplification via PCR is not only dependent on the amount of the gene of interest in the original sample, but it is also majorly influenced by the primers' ability to bind on the single stranded DNA; in this case, amplification with the 3′c primer is more effective than with the 3′a or 3′b primer. This suggests that these 3′ primers are less capable of binding to the single stranded DNA than the 3′c primer. A possible cause for this difference in annealing efficiency is the thymine and adenine rich section which occurs in both, the 3′a and 3′b primer sequence; as it can lead to the formation of primer dimers due to inter-primer homology as shown in Figure 12, rather than annealing to the DNA single strand.

Figure 12 Inter-primer homologies that can occur in the 3′a and 3′b primer leading to less annealing efficiency.

According to these results, standard PCR was conducted, using the 48 h anti-CD3/anti-CD28 stimulation sample as a template, the primer pair 5′b + 3′c, and the Easy-A polymerase for amplification. The PCR product was separated by gel electrophoresis; but no band was detectable at 550 bp (data not shown). This evidence led to the conclusion that stimulation with anti-CD3 and anti-CD28 over a period of 48 h indeed leads to increased *RANKL* expression, however it is not enough to be amplified efficiently with the used methods.

As discussed, murine T-cells express *RANKL in vitro* after the stimulation with just anti-CD3 and no additional anti-CD28. It was suggested that the same may apply to human T-cells, which was tested by preparing two Jurkat cultures: one supplemented with anti-CD3, one with 1 µg mL^{-1} the other with 10 µg mL^{-1}. Samples from both cultures were withdrawn after 24 h and 48 h and total RNA was extracted. RT was performed and control RT reactions were implemented with additional DTT in order to exclude the possibility of the formation of secondary RNA structures that could constrain the transcription reaction. Subsequently, two PCR reactions were conducted using GoTaq and Easy-A, respectively; the resulting gels are shown in Figure 13.

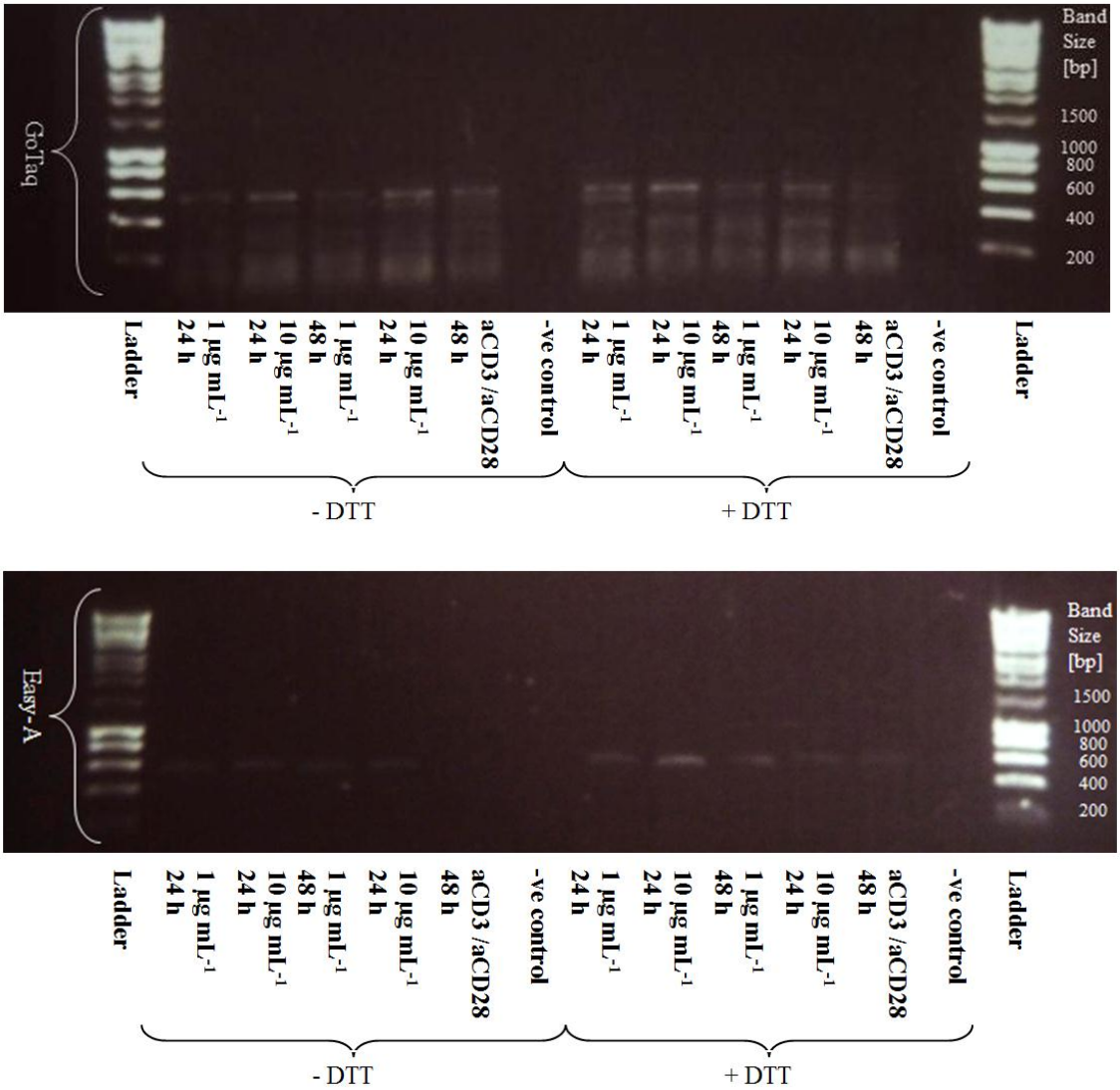

Figure 13 Jurkat cells were cultivated for 48 h in the presence of anti-CD3. Additionally, RNA samples of Jurkat cells that had grown in the presence of 1.1 µg mL^{-1} anti-CD3 and 0.5 µg mL^{-1} anti-CD28 for 48 h and a negative control were prepared. RT was performed with and without addition of DTT. The following PCR took place with GoTaq (top gel) and Easy-A polymerase (bottom gel). Successful amplification of *RANKL* resulted in a band at approximately 550 bp.

By comparing both gels, a significant difference between GoTaq and Easy-A polymerase is evident, although both reactions and electrophoreses were performed simultaneously under the same environmental circumstances. GoTaq polymerase produces a sufficient amount of PCR product that leads to clearly visible but smeared bands. Its error rate of 8×10^{-6} errors bp^{-1} $duplication^{-1}$ is relatively high compared to Easy-A, which, as a high-fidelity polymerase, possesses an error rate six times lower than GoTaq (Agilent Technologies). For this reason Easy-A polymerase is more suitable for amplifying a gene that is destined to be cloned into another organism. The increased proofreading ability of Easy-A leads not only to a lower mutation rate but also to less unspecific amplification products, which is why the resulting bands do not show any smears. They are however relatively pale in comparison to the bands resulting from PCR with GoTaq polymerase, possibly because of comparatively lower enzyme activity. Stimulation with anti-CD3 indeed leads to a noticeable expression of *RANKL* in Jurkat cells, which can be determined as a band the size of approximately 550 bp.

The higher anti-CD3 concentration of 10 µg mL^{-1} resulted in more intense bands than 1 µg mL^{-1} anti-CD3, but there was no significant difference between 24 h and 48 h of stimulation. Addition or absence of DTT does not have any significant effect, meaning that *RANKL* mRNA is not likely to form noticeable secondary structures. For more precise predications concerning the impact of anti-CD3 concentration and exposure time on *RANKL* expression in Jurkat cells, a more extensive experiment would be necessary that evaluates wider ranges of both parameters. For the purpose of this work however, the successful amplification of *RANKL* with the Easy-A polymerase was sufficient.

4.2 Cloning and Transformation of the RANKL Gene

Once *RANKL* was successfully amplified, the resulting PCR product could be used directly for cloning into the expression vector and the following transformation of *E. coli*. As the optimal amount of PCR product for the cloning reaction was not specified in the user manual of the pSecTag/FRT/V5-His TOPO® TA Expression Kit, two different reactions were performed, with one reaction mix containing 1 µL PCR product and the other mix containing 3 µL. Both reaction mixes were otherwise treated equally and used for transformation. From each transformation, two different volumes, 50 µL and 200 µL, were spread on agar plates, in order to ensure that at least one plate had well-spaced colonies.

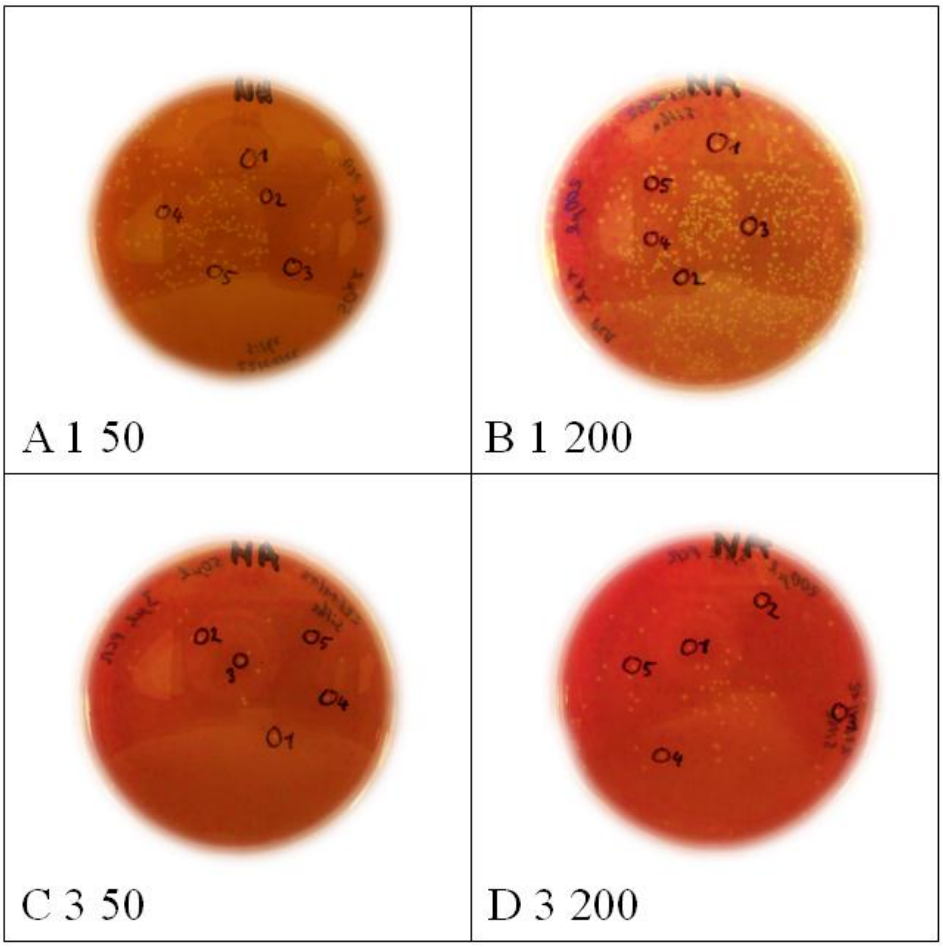

Figure 14 Nutrient agar plates with plated transformants after 24 h incubation at 37 °C. A: 1 µL PCR product, 50 µL spread (1 50). B: 1 µL PCR product, 200 µL spread (1 200). C: 3 µL PCR product, 50 µL spread (3 50). D: 3 µL PCR product, 200 µL spread (3 200).

Figure 14 shows the four nutrient agar plates that were named according to the used volumes of PCR product and spread cell suspension 1 50, 1 200, 3 50, and 3 200 after 24 h incubation. The exact number of colony forming units (CFU) for each plate, as well as the transformation efficiency (TE), is shown in Table 2. TE can be determined by dividing CFU by the applied plasmid concentration $c_{Plasmid}$ and the spread volume V_{spread}:

$$TE = CFU\ c_{Plasmid}^{-1}\ V_{spread}^{-1}$$

Table 2 Colony forming units (CFU) and transformation efficiency (TE) per plate after transformation

Nutrient agar plate	CFU [-]	TE [μg^{-1}]
1 50	176	160 000
1 200	681	155 000
3 50	23	20 900
3 200	67	15 200

As logic suggests, the plates containing 200 µL of cell suspension show a noticeably higher colony density than the ones with 50 µL. More interesting is the influence of the used PCR product volume during cloning on TE; in this case, the lower PCR product volume of 1 µL leads to almost 10-fold higher TE. The reason for this difference lies in higher insertion efficiency, which is dependent on the ratio of insert and plasmid. Only a plasmid with successfully inserted *RANKL* changes its state from linear to circular and can then be incorporated by a cell.

Five colonies from each plate were picked and cultivated overnight; in Figure 14, the chosen colonies are marked with black circles. All twenty cultures were named after their plate and a consecutive number, e.g. 1 50 1 for the first picked colony from plate 1 50. The picked clones were cultured in LB medium in order to obtain a sufficient amount of cells for plasmid purification and analysis.

4.3 Analysis of Clones

After purification, all plasmids from the twenty different clones were analysed for the presence and orientation of the *RANKL* insert by performing two PCR reactions with each sample as previously discussed. Figure 15 shows the resulting gels for the plasmids 1 50 1 to 1 200 5, and Figure 16 for the plasmids 3 50 1 to 3 200 5, respectively.

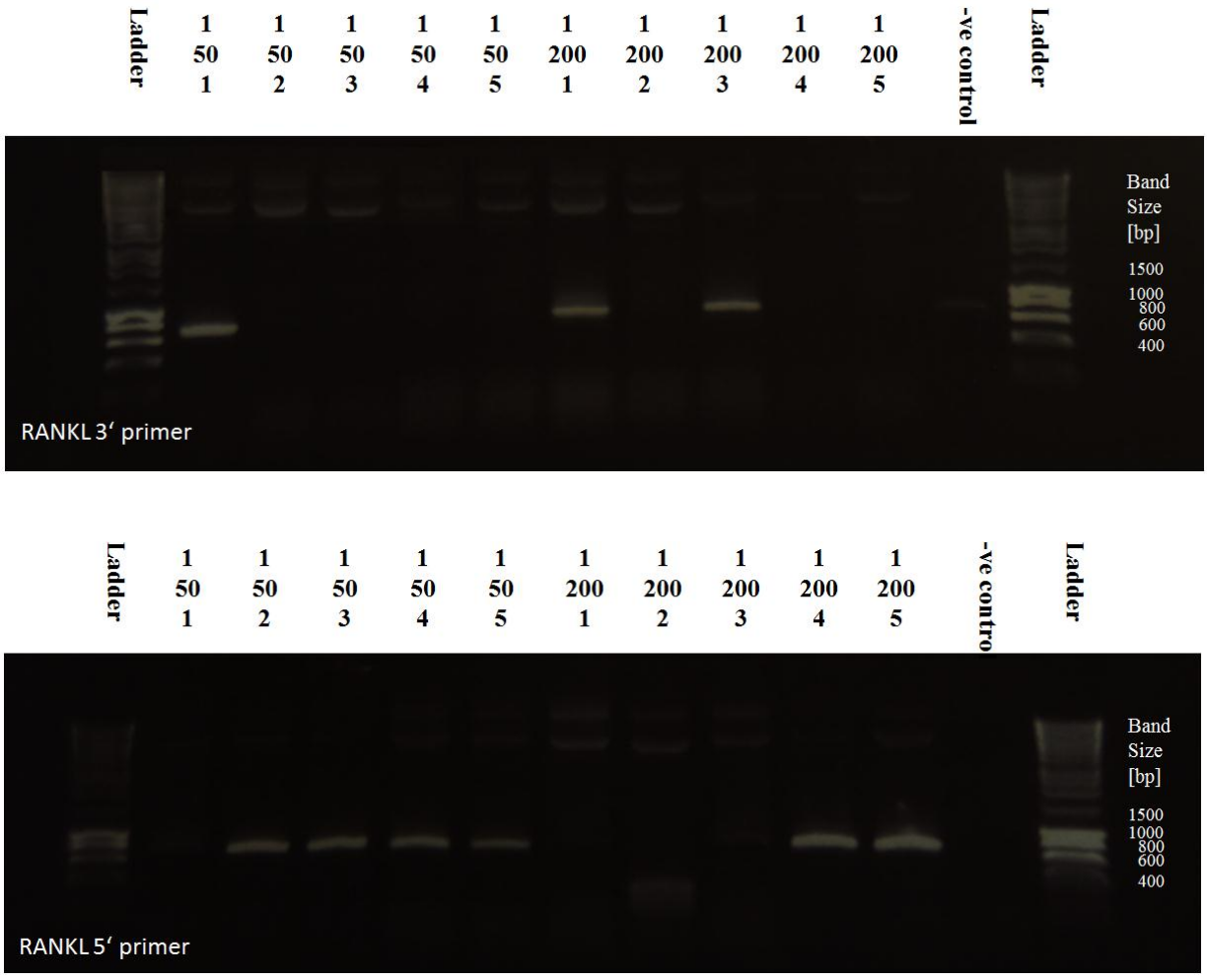

Figure 15 Purified plasmids 1 50 1 to 1 200 5 were amplified by PCR using the forward sequencing primer that is included in the pSecTag/FRT/V5-His TOPO® TA Expression Kit and a *RANKL 3′* primer (top) or 5′ primer (bottom). The bands of each sample in the two gels are complementary to each other; a band at approximately 700 bp in one gel means no band in the other. Correctly included *RANKL* results in a band for the *RANKL 3′* primer combination, an incorrectly inserted gene leads to the reciprocal pattern.

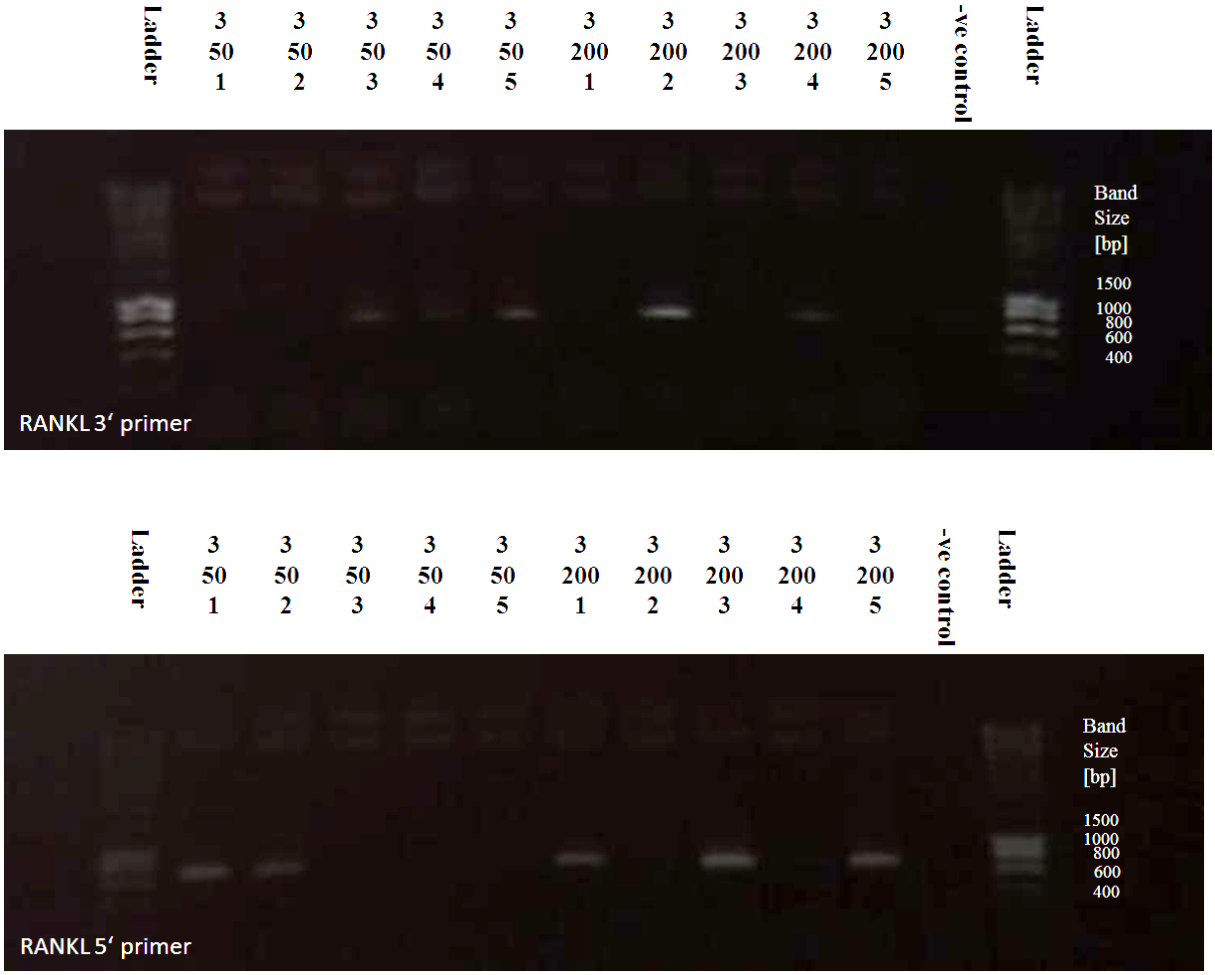

Figure 16 Purified plasmids 3 50 1 to 3 200 5 were amplified by PCR using the forward sequencing primer that is included in the pSecTag/FRT/V5-His TOPO® TA Expression Kit and a *RANKL* 3′ primer (top) or 5′ primer (bottom). The bands of each sample in the two gels are complementary to each other; a band at approximately 700 bp in one gel means no band in the other. Correctly included *RANKL* results in a band for the *RANKL* 3′ primer combination, an incorrectly inserted gene leads to the reciprocal pattern.

As expected, each plasmid shows a specific band pattern that makes it possible to determine the orientation of the inserted *RANKL*. Successful PCR with the forward sequencing primer and the *RANKL* 3′ primer as a reverse primer means that the gene is inserted correctly, i.e., in 5′ 3′ direction. In this case, amplification with the *RANKL* 5′ primer does not lead to a band in the gel, because both priming sequences lie on the same DNA strand. In turn, a gene that was inserted reversely, i.e., in 3′ 5′ direction, can be amplified with the *RANKL* 5′ primer as a reverse primer, PCR with the *RANKL* 3′ primer however, is not successful. This method has the advantage that the result can be controlled easily by comparing both band patterns and it is independent from problems that can occur during restriction digestion analysis. The gels for

samples 1 50 1 to 1 200 5 as shown in Figure 15 feature very sharp bands at a size of 700 bp and an unmistakable band pattern, i.e., there are no bands appearing twice, indicating no sample contamination. Sample 1 200 2 does not show any bands at all, possibly because of failed gene insertion in this particular clone. A less possible explanation is an ineffective transformation; in this case however, the colony must have grown on an antibiotic free spot on the petri dish, which is questionable, as colony 1 200 2 was picked from the centre of the dish (see Figure 14). The gels in Figure 16 with the samples 3 50 1 to 3 200 5 also show unique band patterns, which allow to distinguish between correctly and falsely inserted genes. In both gels, the negative control that was amplified with the *RANKL* 3′ primer shows a weak band at approximately 700 bp; this is most likely due to a contamination which took place during sample preparation. Whereas this is usually a reason to repeat the experiment, it was decided to forgo this step, as no further irregularities in the band patterns were found that indicate DNA contaminations in the samples.

Overall, 8 out of 20 samples possessed a correctly inserted gene, whereas its orientation was inverted in 11 samples and not determinable in 1 sample. The exact results are listed in Table 3.

Table 3 Results of insert orientation analysis. Samples with correctly inserted *RANKL* (5′ 3′ direction) are highlighted green, with falsely inserted (3′ 5′ direction) *RANKL* red, and white when no insert is detectable

Sample	Insert orientation	Sample	Insert orientation	Sample	Insert orientation	Sample	Insert orientation
1 50 1	5′ 3′	1 200 1	5′ 3′	3 50 1	3′ 5′	3 200 1	3′ 5′
1 50 2	3′ 5′	1 200 2	No insert	3 50 2	3′ 5′	3 200 2	5′ 3′
1 50 3	3′ 5′	1 200 3	5′ 3′	3 50 3	5′ 3′	3 200 3	3′ 5′
1 50 4	3′ 5′	1 200 4	3′ 5′	3 50 4	5′ 3′	3 200 4	5′ 3′
1 50 5	3′ 5′	1 200 5	3′ 5′	3 50 5	5′ 3′	3 200 5	3′ 5′

Due to financial limitations, only four samples were sent for sequencing; samples 1 200 1, 1 200 3, 3 200 2, and 3 200 4 were chosen. The received results, each consisting of an overlay of forward and backward sequence, are shown in Figure 17.

A: 1 200 1

```
  1 GAGAAAGCGA TGGTGGATGG CTCATGGTTA GATCTGGCCA AGAGGAGCAA GCTTGAAGCT CAGCCTTTTG
 71 CTCATCTCAC TATTAATGCC ACCGACATCC CATCTGGTTC CCATAAAGTG AGTCTGTCCT CTTGGTACCA
141 TGATCGGGGT TGGGCCAAGA TCTCCAACAT GACTTTTAGC AATGGAAAAC TAATAGTTAA TCAGGATGGC
211 TTTTATTACC TGTATGCCAA CATTTGCTTT CGACATCATG AAACTTCG_G AGACCTAGCT ACAGAGTATC
281 TTCAACTAAT GGTGTACGTC ACTAAAACCA GCATCAAAAT CCCAAGTTCT CATACCCTGA TGAAAGGAGG
351 AAGCACCAAG TATTGGTCAG GGAATTCTGA ATTCCATTTT TATTCCATAA ACGTTGGTGG ATTTTTTAAG
421 TTACGGTCTG GAGAGGAAAT CAGCATCGAG GTCTCCAACC CCTCCTTACT GGATCCGGAT CAGGATGCAA
491 CATACTTTGG GGCTTC_AAA GTTCGAGATA TAGATTGAGC CCCAGTTTTT GGAGTG
```

B: 1 200 3

```
  1 GAGAAAGCGA TGGTGGATGG CTCATGGTTA GATCTGGCCA AGAGGAGCAA GCTTGAAGCT CAGCCTTTTG
 71 CTCATCTCAC TATTAATGCC ACCGACATCC CATCTGGTTC CCATAAAGTG AGTCTGTCCT CTTGGTACCA
141 TGATCGGGGT TGGGCCAAGA TCTCCAACAT GACTTTTAGC AATGGAAAAC TAATAGTTAA TCAGGATGGC
211 TTTTATTACC TGTATGCCAA CATTTGCTTT CGACATCATG AAACTTCAGG AGACCTAGCT ACAGAGTATC
281 TTCAACTAAT GGTGTACGTC ACTAAAACCA GCATCAAAAT CCCAAGTTCT CATACCCTGA TGAAAGGAGG
351 AAGCACCAAG TATTGGTCAG GGAATTCTGA ATTCCATTTT TATTCCATAA ACGTTGGTGG ATTTTTTAAG
421 TTACGGTCTG GAGAGGAAAT CAGCATCGAG GTCTCCAACC CCTCCTTACT GGATCCGGAT CAGGATGCAA
491 CATACTTTGG GGCTTTTAAA GTTCGAGATA TAGATTGAGC CCCAGTTTTT GGAGTG
```

C: 3 200 2

```
  1 GAGAAAGCGA TGGTGGATGG CTCATGGTTA GATCTGGCCA AGAGGAGCAA GCTTGAAGCT CAGCCTTTTG
 71 CTCATCTCAC TATTAATGCC ACCGACATCC CATCTGGTTC CCATAAAGTG AGTCTGTCCT CTTGGTACCA
141 TGATCGGGGT TGGGCCAAGA TCTCCAACAT GACTTTTAGC AATGGAAAAC TAATAGTTAA TCAGGATGGC
211 TTTTATTACC TGTATGCCAA CATTTGCTTT CGACATCATG AAACTTCGGG AGACCTAGCT ACAGAGTATC
281 TTCAACTAAT GGTGTACGTC ACTAAAACCA GCATCAAAAT CCCAAGTTCT CATACCCTGA TGAAAGGAGG
351 AAGCACCAAG TATTGGTCAG GGAATTCTGA ATTCCATTTT TATTCCATAA ACGTTGGTGG ATTTTTTAAG
421 TTACGGTCTG GAGAGGAAAT CAGCATCGAG GTCTCCAACC CCTCCTTACT GGATCCGGAT CAGGATGCAA
491 CATACTTTGG GGCTTTTAAA GTTCGAGATA TAGATTGAGC CCCAGTTTTT GGAGTG
```

D: 3 200 4

```
  1 GAGAAAGCGA TGGTGGATGG CTCATGGTTA GATCTGGCCA AGAGGAGCAA GCTTGAAGCT CAGCCTTTTG
 71 CTCATCTCAC TATTAATGCC ACCGACATCC CATCTGGTTC CCATAAAGTG AGTCTGTCCT CTTGGTACCA
141 TGATCGGGGT TGGGCCAAGA TCTCCAACAT GACTTTTAGC AATGGAAAAC TAATAGTTAA TCAGGATGGC
211 TTTTATTACC TGTATGCCAA CATTTGCTTT CGACATCATG AAACTTCAGG AGACCTAGCT ACAGAGTATC
281 TTCAACTAAT GGTGTACGTC ACTAAAACCA GCATCAAAAT CCCAAGTTCT CATACCCTGA TGAAAGGAGG
351 AAGCACCAAG TATTGGTCAG GGAATTCTGA ATTCCATTTT TATTCCATAA ACGTTGGTGG ATTTTTTAAG
421 TTACGGTCTG GAGAGGAAAT CAGCATCGAG GTCTCCAACC CCTCCTTACT GGATCCGGAT CAGGATGCAA
491 CATACTTTGG GGCTTTTAAA GTTCGAGATA TAGATTGAGC CCCAGTTTTT GGAGTG
```

Figure 17 Sequences of the selected samples with mutations highlighted red. A: 1 200 1 contained two deletions and two substitutions. B: 1 200 3 did not contain any mutations. C: 3 200 2 contained one substitution. D: 3 200 4 did not contain any mutations.

By comparing the sequences from Figure 17 to the original *RANKL* sequence (see Figure 9) it is possible to identify mutations in the form of substitutions, deletions or insertions that have occurred during PCR amplification. In this case, the sequences of the samples 1 200 3 and 3 200 4 were consistent with the original sequence. Sample 1 200 1 contained four mutations: two deletions at the positions 259 and 507, and two substitutions at the positions 258, where guanine instead of adenine, and 506, where cytosine instead of thymine was inserted. Sample 3 200 2 contains one mutation, which is the same substitution at position 258 (guanine instead of adenine) as in sample 1 200 1. The fact that both samples have the same mutation in common suggests that it had occurred in an early stage of the PCR reaction, which led to a carryover into the following reaction products and thus exponential amplification of the mutation with the chance of occurrence of more errors.

4.4 Transfection of CHO Flp-In cells

In accordance with the previous results, the purified plasmids 1 200 3 and 3 200 4 were used for transfection of CHO Flp-In cell cultures, preparing duplicates of each culture. Selection pressure was applied by adding hygromycin B to the growth medium. In Figure 19, the appearance of transfected CHO Flp-In cells growing in selective medium is compared to untransfected cells growing in normal medium, as shown in Figure 18. Typical healthy CHO cells are characterised by their stretched shape and their growth as an adherent monolayer in the tissue culture flask; by visual inspection under an inverted microscope, the light shines through the cells revealing a translucent structure. Dead cells (not shown in Figure 18) can be identified by their shrunken and deflated profile; they appear darker in comparison to healthy cells as the light is not able to shine through them to the same extent, and they are not attached to the surface of the tissue flask, but float in the medium.

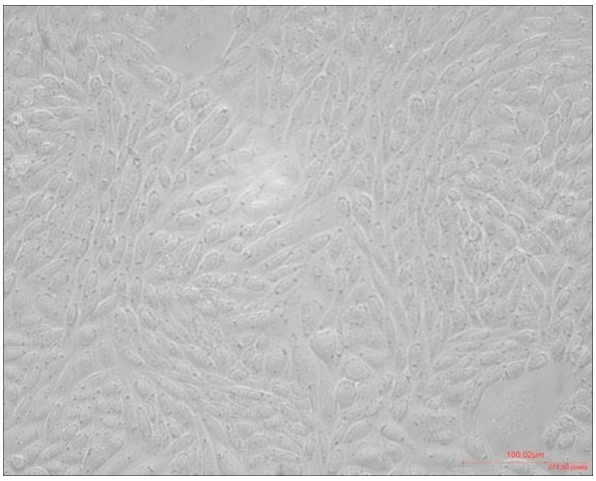

Figure 18 Untransfected CHO Flp-In cells growing in non-selective medium.

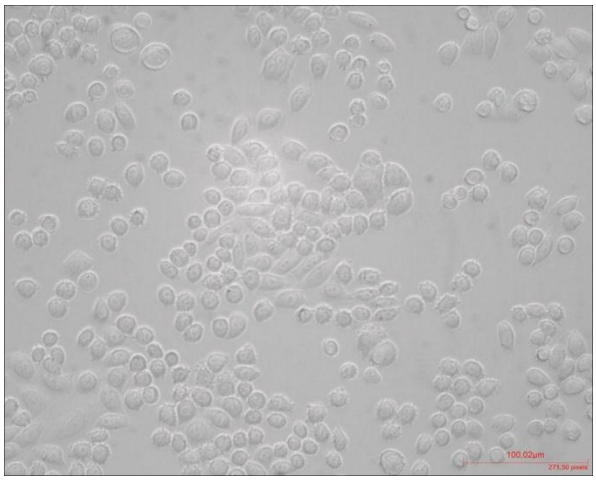

Figure 19 Transfected CHO Flp-In cells after three weeks of selection with hygromycin B.

Figure 19 shows the culture of transfected CHO Flp-In cells after three weeks of growth in selective medium. Compared to normal cells, they differed particularly in their shape, as most of them are round instead of elongated; however, they were still attached to the surface, translucent, and of the right size. Nevertheless, the fact that they rounded up indicates that they were not entirely healthy, which was most likely due to the high hygromycin B concentration. Another consideration is that their affected health was connected to their secretion of RANKL, as the protein belongs to the TNF family, which is known to be associated with apoptosis (Rath and Aggarwal, 1999).

These considerations were tested by removal of hygromycin B from the medium; interestingly, the cells showed an increased apoptosis rate as soon as a the non-selective medium was added and it was necessary to change the medium daily due to high levels of cell debris floating in the medium. This phenomenon was possibly caused by a defence mechanism; when selection pressure is applied by adding hygromycin B to the cell culture, some cells did not die off, but entered the G0 phase, in which the cells existed in an inactive state unable to proliferate. After releasing the selection pressure the cells may not have been able to re-enter the cell cyclus, but apoptosis was triggered.

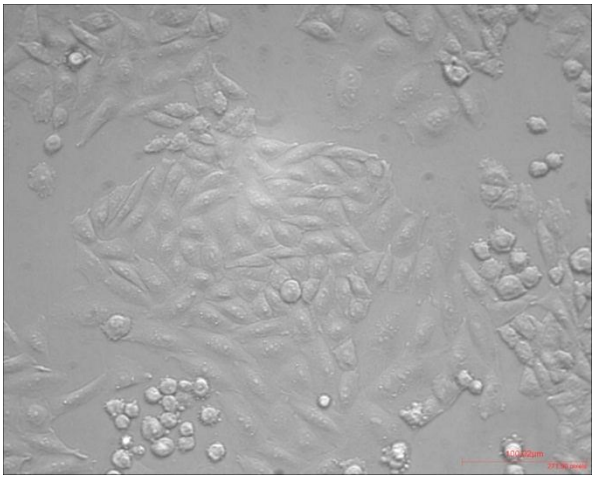

Figure 20 Transfected CHO Flp-In cells after growing in non-selective medium for three days.

The physical appearance after three days of growth in non-selective growth medium is shown in Figure 20. The cells had visibly recovered; most of them were spread down and resembled the healthy CHO Flp-In cells in Figure 18, and only few showed ailing or even apoptotic characteristics. This evidence disagrees about the previously depicted concerns the presence of RANKL could affect the cells' health negatively. More probable is that the unsound characteristics are due to the presence of hygromycin B. For further analysis of presence and concentration of secreted RANKL, supernatants were supplemented again with the antibiotic; furthermore, an amount of transfected cells were harvested and stored at −80 °C prior to further use.

4.5 Determination of RANKL in Supernatants of Transfected CHO Flp-In cells

Due to its integration in the previously described vector next to the Igκ secretion signal, the product RANKL is supposed to be secreted into the medium. Consequently, qualitative RANKL analysis was conducted in supernatants of transfected CHO Flp-In cultures after three days of growth in fresh medium. As the product concentration could not be estimated, the experiment was conducted using the centrifuged supernatants and acetone precipitates of the same samples. Together with the samples, a protein ladder with known protein sizes and concentration was analysed, which allowed to determine the sizes of the separated proteins.

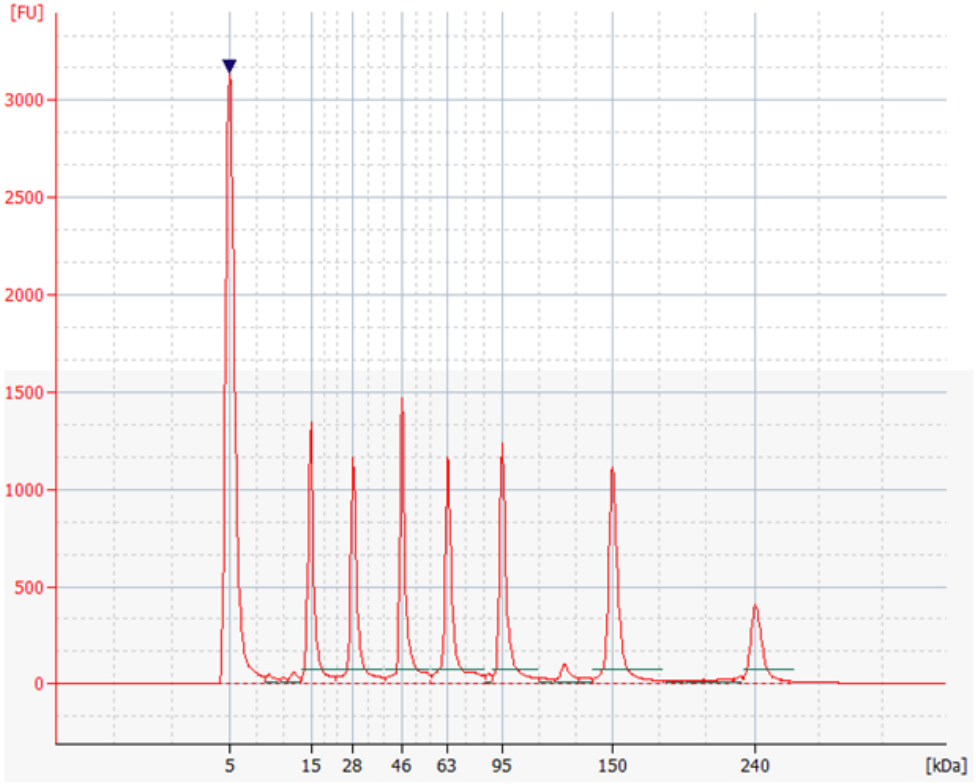

Figure 21 Electropherogram of the protein ladder separated by the 2100 Bioanalyzer consists of a lower marker (5 kDa) and seven ladder peaks.

Figure 21 shows a typical electropherogram of the separated protein ladder; this separation not only serves for determination of a specific protein, but also as a control if protein labelling and handling of the chip was successfully conducted. Sample preparation and experimental procedure are correct due to the electropherogram in Figure 21 showing seven well separated peaks with an additional lower marker peak at 5 kDa. The lower marker peak appears in every sample as it represents a fluorescent dye which is part of the sample buffer; the abscissa of each following sample electropherogram is furthermore labelled with the size of the ladder proteins.

Figure 22 shows an overlay of two electropherograms, an analysed supernatant of untransfected CHO Flp-In cells (negative control, green) and the same sample spiked with 50 µM RANKL (positive control, red). As previously clarified, RANKL has a size of 31 kDa and is therefore expected to migrate shortly after the second ladder peak.

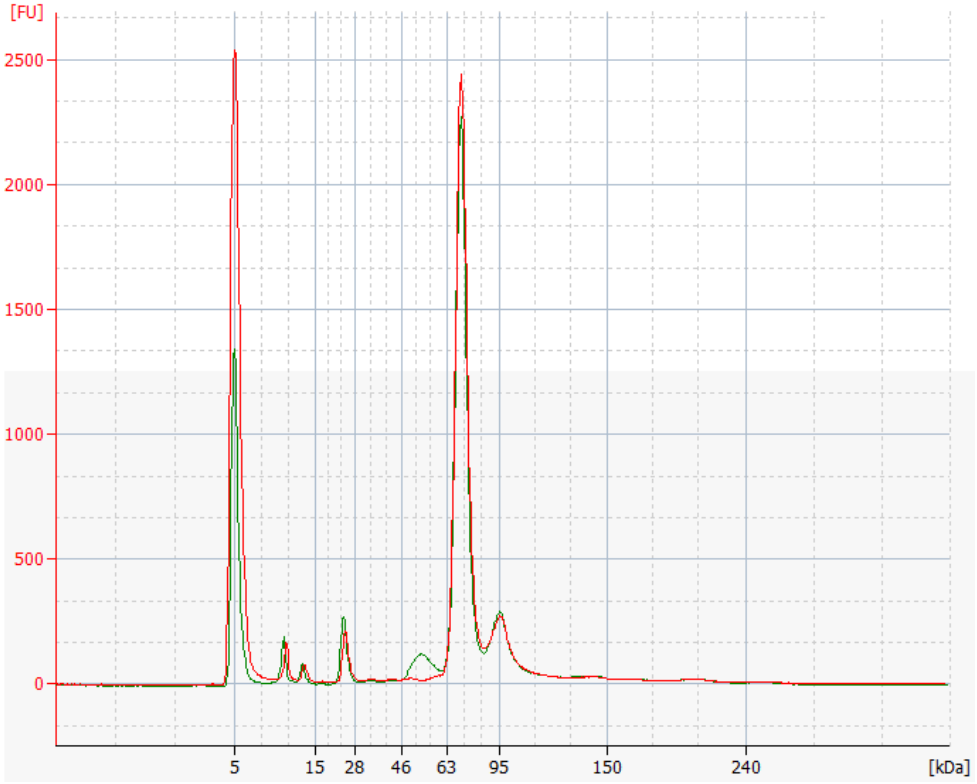

Figure 22 Overlay of two electropherograms. A negative control (green), consisting of the supernatant of untransfected CHO Flp-In cells and a positive control (red), consisting of the same sample spiked with 50 µM RANKL.

Both electropherograms in Figure 22 show five clearly distinguishable peaks, most prominent of all is a peak at 71 kDa; this peak represents bovine serum albumin (BSA), which has a size of 66 kDa, and is one of the main components of FBS, in turn a component of the used medium. The negative control sample shows another peak shortly before the BSA peak, which may be due to partial BSA degradation or a sample contamination. Despite the high concentration of 50 µM, the positive control sample does not show a peak that differs from the peak pattern of the negative control sample, which would be in agreement with the size of RANKL; also, the repetition of the experiment using a freshly prepared positive control sample did not lead to a different result. Interestingly, the lower marker peak in the positive control sample is approximately twice has high as in the negative control sample, it was therefore suggested that RANKL migrates as a much smaller protein of approximately 5 kDa, which results in a merging of lower marker and RANKL peak. However, this would mean a size decrease of more than 80 % compared to the original size of 31 kDa, which is

improbable. It is more likely that the differences in lower marker peak size are due to different amounts of excess marker that remained in the sample after the labelling reaction.

Another suggestion was that RANKL interacted with BSA and was therefore not visible as a separate peak. For this reason, a serial dilution of RANKL in PBS was analysed on the 2100 Bioanalyzer; Figure 23 shows an electropherogram of the highest applied concentration, which was 10 µM. Again, there was no visible peak at 31 kDa, but only the lower marker peak, which was also the case for the higher applied dilutions (data not shown). Accordingly, the fact that RANKL could not be determined in the positive control sample is not associated with interactions with medium components, otherwise it would have been determinable in this case. These results led to the conclusion that the difficulties in RANKL determination must be related to the protein itself.

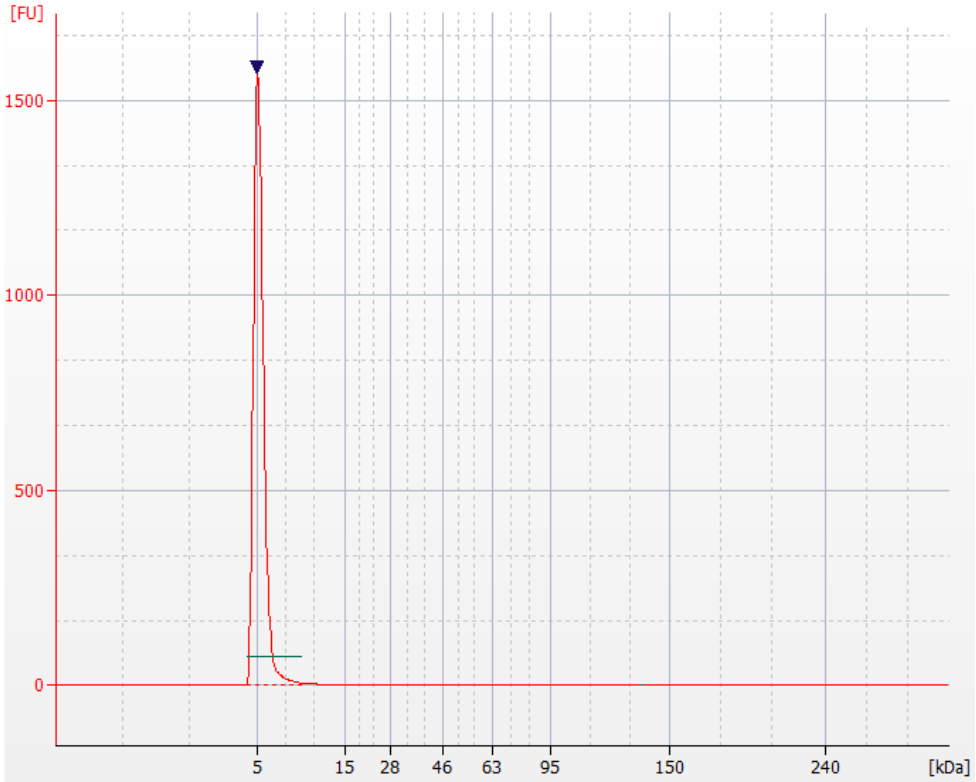

Figure 23 Electropherogramm of 10 µM RANKL diluted in PBS.

As previously depicted, the detection of proteins in the 2100 Bioanalyzer is based on a prior labelling reaction, where lysine amino acids in the protein are labelled with a fluorescent dye. RANKL contains 12 lysine amino acids, almost 7 % of the amino acid sequence, which consists of 175 amino acids in total; it is possible that this lysine content is not sufficient for an adequate labelling reaction, resulting in invisibility for the detector. In order to check this idea, it was suggested to repeat the experiment with a serial dilution of the 19.5 kDa sized INF-α, which contains 9 lysine amino acids or 5.5 % of the complete sequence. Analysis of the resulting electropherograms (not shown) indeed revealed difficulties concerning the detection of IFN-α, as it was only detectable at concentrations > 1 mM, and not visible separately, but merged with the lower marker peak. These findings confirm the previous idea RANKL may not be detectable by this lab-on-a-chip method due to its small size and lysine content; however, they contradict the description of the Agilent High Sensitivity Protein 250 Kit which promises successful separation of proteins between 10 and 250 kDa. Another possible explanation for the detection problem is that an error could have occurred during preparation of the RANKL aliquot that was used for all analyses with the 2100 Bioanalyzer; however, as this step was not undertaken in the local laboratories, it was not possible to reconstruct the aliquots and draw conclusions regarding their correctness. Assuming that this was the case, as other conceivable possibilities were disproved, further analysis of the supernatants of transfected CHO Flp-In cells was conducted nonetheless.

Figure 24 shows an overlay of two electropherograms of supernatants of transfected CHO Flp-In cells, samples were prepared by centrifuging the supernatants (blue) and subsequently performing an acetone precipitation (red) in order to concentrate proteins in the sample. The peak pattern that results from the simple sample preparation resembles in most instances the negative control peak pattern in Figure 22, indicating that no RANKL is detectable in this sample.

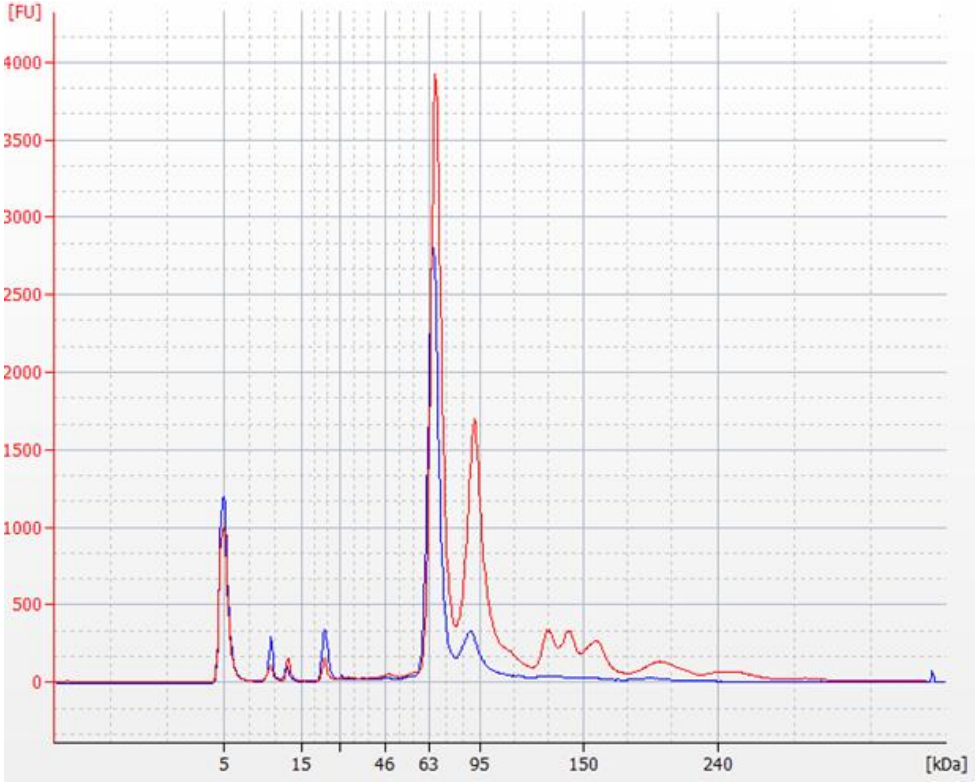

Figure 24 Electropherograms of an analysed supernatant of a culture of transfected CHO Flp-In cells. Sample preparation consisted of simple centrifugation (blue) with subsequent acetone precipitation (red) respectively.

Both electropherograms show the lower marker peak at 5 kDa, as well as three peaks in the area between 10 and 28 kDa; most prominent is the BSA peak at 71 kDa followed by a second peak. As expected, the acetone precipitated sample shows higher peaks for these two proteins due to the higher concentration after precipitation, and a peak triplet in the area between 130 and 170 kDa that does not appear in the electropherogram of the not precipitated sample. The fact that no peak for RANKL could be found led to the assumption that the RANKL concentration in the culture supernatant may not be high enough to be detected by this method; furthermore, concentrations of BSA and other medium compounds may be too high and therefore overtopping the low RANKL concentrations. For this reason, samples were prepared using an immunoprecipitation method, in which RANKL was systematically separated from other medium compounds by precipitating it by means of a specific antibody.

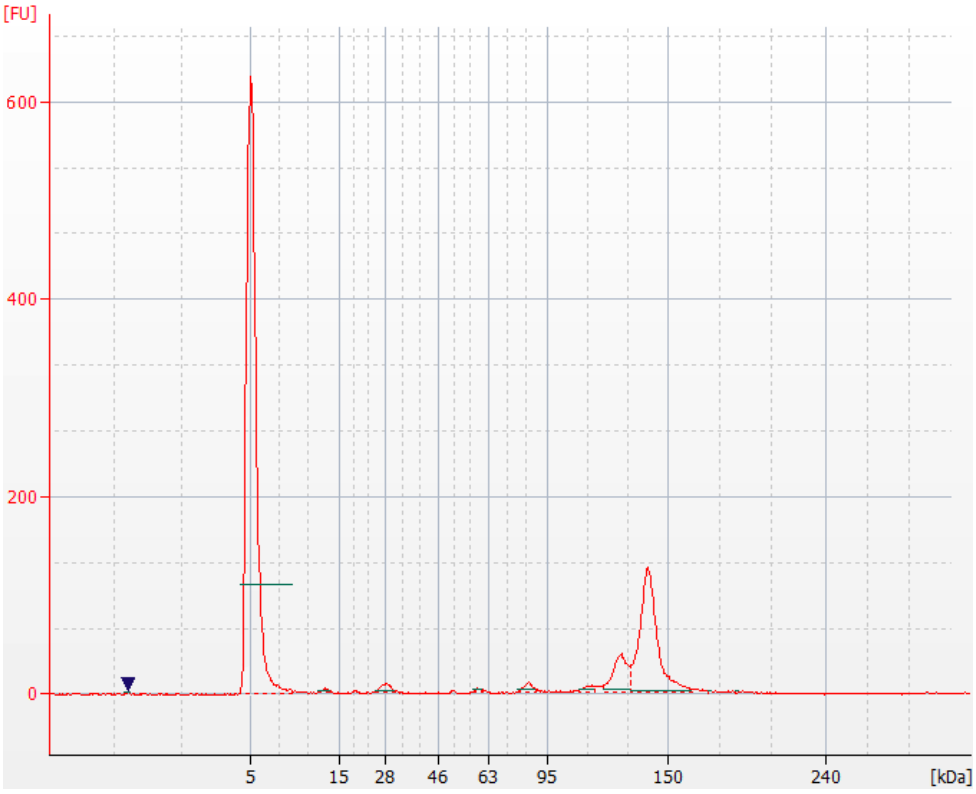

Figure 25 Electropherogram of an analysed supernatant of a culture of transfected CHO Flp-In cells. Sample preparation consisted of centrifugation, labelling reaction and subsequent immunoprecipitation in order to concentrate RANKL.

Figure 25 shows the electropherogram resulting from immunoprecipitation of a labelled supernatant sample. In comparison to Figure 24, this electropherogram shows a different peak pattern. Since the sample was immunoprecipitated with respect to RANKL, there should not be any further peak than one at 31 kDa however it is possible that not all additional proteins were washed out during the immunoprecipitation of RANKL. Furthermore, the lower marker peak is still visible, which is also due to insufficient washing, serendipitously this peak is necessary for verification of the labelling reaction. With this sample preparation consisting of centrifugation, labelling reaction, and immunoprecipitation, it was ultimately possible to detect a peak that appeared at 29 kDa; the probability that this peak represents RANKL is high, since no such peak was observed for the formerly conducted sample preparation methods. The presumptive RANKL peak covers a relatively small area, indicating that the RANKL concentration in the supernatant of the transfected CHO Flp-In cells is not considerably high. As previously discussed, the health of the used cultures was significantly

affected by the addition of hygromycin B to the growth medium; it is therefore likely that gene expression in these cells was altered and protein secretion was suppressed. Two further peaks are visible at 132 kDa and 144 kDa; as RANKL was precipitated by means of a specific antibody, it is possible that these peaks represent a RANKL-anti-RANKL complex. The possibility that they result from the antibody without RANKL can be eliminated as the labelling reaction was conducted before the antibody was added, meaning that the antibody itself could not have been detected.

5. Summary, Conclusions and Future Prospects

Osteoarthritis was long time considered to be an ordinary symptom of old age, caused by a lifelong use of joints and therefore abrasion of cartilage and bone, and although OA is prevalent among elder people, it has become clear during the last twenty years that far more factors contribute to the disease than sheer age (Sharma and Kapoor, 2007). A critical role in the development and progress of OA is ascribed to a malfunction of osteoclasts, either concerning their differentiation or their function itself (Karsenty and Wagner, 2002). In order to investigate to what extend and in which exact way this cell type contributes to the disease, it is still necessary to conduct further studies on the characteristics of osteoclasts and osteoclastogenesis including receptors, transcription factors and signalling molecules that are involved in the process. RANKL is a member of the TNF family and is known to play a decisive role in osteoclast differentiation; by binding to its receptor RANK, it induces a signalling cascade that finally leads to the differentiation of haematopoietic stem cells to osteoclasts. For *in vitro* osteoclastogenesis pluripotent monocytes, derived from human blood, can be cultured in the presence of RANKL and M-CSF in order to obtain osteoclasts (Khosla, 2001). The aim, CMS is currently concentrating on, is to find out the effect, PAR-2 on the surface of osteoclasts is having in OA development and progression; for this purpose, the group cultures osteoclasts and requires therefore great amounts of RANKL.

The aim of this work was to produce and subsequently identify RANKL. For this purpose a selection of leukaemic cell lines was screened for the expression of *RANKL*, the gene was then isolated, amplified and cloned into an expression vector. After transformation of *E. coli* with the plasmid and subsequent analysis of clones in terms of gene orientation and sequence, CHO Flp-In cells were transfected with the purified plasmid gained from a successfully transformed *E. coli* colony. The transfected cells were selected by applying selection pressure

and the secreted protein was identified using a novel lab-on-a-chip method based on electrophoresis.

In addition to the primary aim of this work, interesting insights concerning *RANKL* expression in human leukaemic cell lines were achieved; as Jurkat cells are T-cells, they are expected to express *RANKL in vivo* (Wong et al., 1997), by cultivation *in vitro* however, expression levels are not significantly high, it is in fact difficult to determine *RANKL* via qRT-PCR. Expression can be increased considerably by stimulation with the antibodies anti-CD3 and anti-CD28 over a period of 48 h; stimulation with only anti-CD3 leads to even higher expression levels, as it is also the case in murine T-cells (Josien et al., 1999; Wang et al., 2002).

The choice of a suitable primer pair is crucial for the successful amplification of the gene, as thymine and adenine rich regions near the stop codon increase the risk of inter-primer homologies when the primer sequences incorporate these regions. The previous findings concerning *RANKL* expression in unstimulated and anti-CD3/anti-CD28 stimulated Jurkat cells, must therefore be considered carefully, as a less suitable primer pair was used for the corresponding PCR reactions.

In terms of transformation, an interesting approach concerning clone analysis was established by using a PCR based method. By combining a primer that is complementary to a sequence in the plasmid, in this case the T7 sequencing primer that is included in the used expression kit, with either the 5′ or 3′ primer of the cloned gene, it is possible to generate a band pattern which allows conclusions concerning the insert orientation. This technique proved to be at least as effective, if not more so, than the classical restriction digestion analysis, as it is easily realisable with standard PCR equipment and reagents. Beyond that, no intricate restriction digest fragment analysis has to be prepared as it is sufficient to estimate the expected size of the resulting PCR product.

CHO Flp-In cells were chosen for transfection and consequently production of RANKL, as CHO is a well-established cell line especially in terms of production of recombinant proteins, furthermore this cell line is generally of robust health and it is unpretentious with respect to maintenance and care (Kim et al., 2012). The CHO Flp-In cell line is equipped with an FRT site, which enables integration of a gene of interest, in this case *RANKL*, into the genome. After transfection, difficulties related to the applied selection pressure occurred, as the high antibiotic concentration that was necessary to ensure successful selection affected the culture negatively. Initial concerns this may be connected with the presence of RANKL in the medium were disproved, as the cells visibly recovered after elimination of the selection pressure.

Determination of the final product RANKL was conducted using a novel lab-on-a-chip method, which helped with characterising and establishing the 2100 Bioanalyzer and the associated protein separation method at CMS. Using this method combined with an antibody based immunoprecipitation, RANKL could be determined in the supernatant of transfected CHO Flp-In cells; however the detectable concentration was unexpectedly low, which was probably due to side effects of the treatment with hygromycin B, which can modify gene expression and secretion patterns. In order to further characterise the expression and secretion behaviour, it is still necessary to conduct further tests, for instance by growing the culture without selection pressure or analysing cell lysates in addition to the supernatants, as difficulties concerning secretion of the protein may occur in the cells. It is furthermore recommended to create monoclonal cultures to ensure consistency of expression levels and thus a predictable protein concentration in the supernatant.

The final purpose for this recombinant RANKL is the application for *in vitro* osteoclastogenesis; due to unforeseen restrictions however, it was not possible to test the protein for its ability to induce differentiation of monocytes into osteoclasts. This is an

important step in the development that still needs to be conducted in order to be able to draw conclusions as to whether the recombinant RANKL has the same features and allows equal differentiation efficiency as the purchased protein.

References

Agilent Technologies
Easy-A High-Fidelity PCR Cloning Enzyme
Instruction Manual, Revision B

Anderson, D.M.; Maraskovsky, E.; Billingsley, W.L.; Dougall, W.C.; Tometsko, M.E.; Roux, E.R.; Teepe, M.C.; DuBose, R.F.; Cosman, D.; Galibert, L. (1997)
A homologue of the TNF receptor and its ligand enhance T-cell growth and dendritic-cell function
In: Nature. Vol. 390 pp 175-179

Ausubel, F.M.; Brent, R.; Kingston, R.E.; Moore, D.D.; Seidman, J.G.; Smith, J.A.; Struhl, K. (1999)
Basic Protocol 1: Alkaline Lysis Miniprep
In: *Short Protocols in Molecular Biology: A Compendium of Methods from Current Protocols in Molecular Biology.* 4th edition. Chapter 1.6 USA: John Wiley & Sons

Felgner, P.L.; Gadek, T.R., Holm, M.; Roman, R.; Chan, H.W.; Wenz, M.: Northrop, J.P.; Ringold, G.M.; Danielsen, M. (1987)
Lipofection: A highly efficient, lipid-mediated DNA-transfection procedure
In: Proceedings of the National Academy of Sciences of the United States of America. Vol. 84 pp 7413-7417

Felson, D.T. (2003)
Epidemiology of osteoarthritis
In: Brandt, K.D.; Doherty, M.; Lohmander, L.S. – *Osteoarthritis.* 2nd Edition.
New York: Oxford University Press

Ferrell, W.R.; Lockhart, J.C.; Kelso, E.B.; Dunning, L.; Plevin, R.; Meek, S.E.; Smith, A.J.H.; Hunter, G.D.; McLean, J.S.; McGarry, F.; Ramage, R.; Jiang, L.; Kanke, T.; Kawagoe, J. (2003)
Essential role for proteinase-activated receptor-2 in arthritis
In: The Journal of Clinical Investigation. Vol. 111 pp 35-41

Flores, R.H.; Hochberg, M.C. (2003)
Definition and classification of osteoarthritis
In: Brandt, K.D.; Doherty, M.; Lohmander, L.S. – *Osteoarthritis.* 2nd Edition.
New York: Oxford University Press

Freeburn, R.W. (2012)
Personal communication

Goldring, M.B. (2000)
The Role of the Chondrocyte in Osteoarthritis
In: Arthritis and Rheumatism. Vol. 43 pp 1916-1926

Hayami, T.; Pickarski, M.; Wesolowski, G.A.; Mclane, J.; Bone, A.; Destefano, J.; Rodan, G.A.; Duong, L.T. (2004)
The Role of Subchondral Bone Remodeling in Osteoarthritis
In: Arthritis & Rheumatism. Vol. 50 pp 1193-1206

Heinegård, D.; Bayliss, M.; Lorenzo, P. (2003)
Biochemistry and metabolism of normal and osteoarthritic cartilage
In: Brandt, K.D.; Doherty, M.; Lohmander, L.S. – *Osteoarthritis.* 2nd Edition.
New York: Oxford University Press

Henriksen, K.; Bollerslev, J.; Everts, V.; Karsdal, M.A. (2011)
Osteoclast Activity and Subtypes as a Function of Physiology and Pathology – Implications for Future Treatments of Osteoporosis
In: Endocrine Reviews. Vol. 32(1) pp 31-63

Hsu, H.; Lacey, D.L.; Dunstan, C.R.; Solovyev, I.; Colombero, A.; Timms, E.; Tan, H.L.; Elliott, G.; Kelley, M.J.; Sarosi, I.; Wang, L.; Xia, X.Z.;Elliot, R.; Chiu, L.; Black, T.; Scully, S.; Capparelli, C.; Morony, S.; Shimamoto, G.; Bass, M.B.; Boyle, W.J. (1999)
Tumour necrosis factor receptor family member RANK mediates osteoclast differentiation and activation induced by osteoprotegerin ligand
In: Proceeding of the National Academy of Sciences of the United States of America. Vol. 96(7) pp 3540-3545

Josien, R.; Wong, B.R.; Li, H.-L.; Steinman, R.M.; Choi, Y. (1999)
TRANCE, a TNF Family Member, Is Differentially Expressed on T Cell Subsets and Induces Cytokine Production in Dendritic Cells
In: The Journal of Immunology. Vol. 162 pp 2562-2568

Karsenty, G.; Wagner, E.F. (2002)
Reaching a Genetic and Molecular Understanding of Skeletal Development
In: Developmental Cell. Vol. 2 pp 389-406

Karsenty, G. (1999)
The genetic transformation of bone biology
In: Genes & Development. Vol. 13 pp 3037-3051

Khosla, S. (2001)
Minireview: The OPG/RANKL/RANK System
In: Endocrinology. Vol. 142(12) pp 5050-5055

Kim, J.Y.; Kim, Y.-G.; Lee, G.M. (2012)
CHO cells in biotechnology for production of recombinant proteins: current state and further potential
In: Applied Microbiology and Biotechnology. Vol. 93 pp 917-930

Kingston, B. (2001)
Understanding Joints 2nd Edition
Cheltenham, UK: Nelson Thornes Ltd

Kodama, H.; Nose, M.; Niida, S.; Yamasaki, A. (1991)
Essential role of macrophage colony-stimulating factor in the osteoclast differentiation supported by stromal cells
In: The Journal of Experimental Medicine. Vol. 173(5) pp 1291-1294

Life Technologies (2010)
pSecTag/FRT/V5-His TOPO® TA Expression Kit
User Manual, Version E

Logan, J.; Edwards, K.; Saunders, N. (2009)
Real-time PCR – Current Technology and Applications
Norfolk, UK: Caister Academic Press

Poole, R.; Guilak, F.; Abramson, S.B. (2007)
Etiopathogenesis of Osteoarthritis
In: Moskowitz, R.W.; Altman, R.D.; Hochberg, M.C.; Buckwalter, J.A.; Goldberg, V.M. *Osteoarthritis Diagnosis and Medical/Surgical Management.* 4th Edition. Philadelphia: Lippincott Williams & Wilkins

Rath, P.C.; Aggarwal, B.B. (1999)
TNF-Induced Signaling in Apoptosis
In: Journal of Clinical Immunology. Vol. 19 pp 350-364

Ross, C. (1997)
A comparison of osteoarthritis and rheumatoid arthritis: diagnosis and treatment
In: The Nurse practitioner. Vol. 22 pp 23-24

Schneider, U.; Schwenk, H.; Bornkamm, G. (1977)
Characterization of EBV-genome negative "null" and "T" cell lines derived from children with acute lymphoblastic leukemia and leukemic transformed non-Hodgkin lymphoma
In: International Journal of Cancer. Vol. 19 pp 621-626

Sharma, L.; Kapoor, D. (2007)
Epidemiology of Osteoarthritis
In: Moskowitz, R.W.; Altman, R.D.; Hochberg, M.C.; Buckwalter, J.A.; Goldberg, V.M. *Osteoarthritis Diagnosis and Medical/Surgical Management.* 4th Edition. Philadelphia: Lippincott Williams & Wilkins

Simonet, W.S.; Lacey, D.L.; Dunstan, C.R.; Kelley, M.; Chang, M.S.; Lüthy, R.; Nguyen, H.Q.; Wooden, S.; Bennett, L.; Boone, T.; Shimamoto, G.; DeRose, M.; Elliott, R.; Colombero, A.; Tan, H.L.; Trail, G.; Sullivan, J.; Davy, E.; Bucay, N.; Renshaw-Gegg, L.; Hughes, T.M.; Hill, D.; Pattinson, W.; Campbell, P.; Sander, S.; Van, G.; Tarpley, J.; Derby, P.; Lee, R.; Boyle, W.J. (1997)
Osteoprotegerin: a novel secreted protein involved in the regulation of bone density
In: Cell. Vol. 89(2) pp 309-319

Smith, R.; Ransjö, M.; Tatarczuch, L.; Song, S.; Pagel, C.N.; Morrison, J.R.; Pike, R.N.; Mackie, E.J. (2004)
Activation of Protease-Activated Receptor-2 Leads to Inhibition of Osteoclast Differentiation
In: Journal of Bone and Mineral Tissue Research. Vol. 19(3) pp 507-516

Soysa, N.S.; Alles, N. (2009)
NF-κB functions in osteoclasts
In: Biochemical and Biophysical Research Communication. Vol. 378 pp 1-5

Takayanagi, H. (2007)
The Role of NFAT in Osteoclast Formation
In: Annals of the New York Academy of Sciences. Vol. 1116 pp 227-237

Wang, R.; Zhang, L.; Xiaoren, Z.; Moreno, J.; Celluzzi, C.; Tondravi, M.; Shi, Y. (2002)
Regulation of activation-induced receptor activator of NF-κB ligand (RANKL) expression in T cells
In: European Journal of Immunology. Vol. 32 pp 1090-1098

Wenz, C.; Rüfer, A. (2010)
Immunoprecipitation and the High Sensitivity Protein 250 Assay
In: BioTechniques. Vol. 48 pp 330-332

WHO (2008)
The global burden of disease: 2004 update
World Health Organization

Wong, B.R.; Josien, R.; Lee, S.Y.; Sauter, B.; Li, H.; Steinman, R.M.; Choi, Y. (1997)
TRANCE (tumor necrosis factor [TNF]-related activation-induced cytokine), a new TNF family member predominantly expressed in T cells, is a dendritic cell-specific survival factor
In: The Journal of Experimental Medicine. Vol. 186(12) pp 2075-2080

Xing, L.; Schwarz, E.M.; Boyce, B.F. (2005)
Osteoclast precursors, RANKL/RANK, and immunology
In: Immunological Reviews. Vol. 208 pp 19-29

Zhu, X.-D.; Sadowski, P.D. (1995)
Cleavage-dependent Ligation by the FLP Recombinase – Characterization of a Mutant FLP Protein with an Alteration in Catalytic Amino Acid
In: The Journal of Biological Chemistry. Vol. 270 pp 23044-23054